SLAC-PUB-7175
May , 1996

HOME PAGE

http://www.slac.stanford.edu/pubs/icfa/

ICFA INSTRUMENTATION BULLETIN*

The publication of the ICFA Instrumentation Bulletin is an activity of the Panel on Future Innovation and Development of ICFA (International Committee for Future Accelerators).

• Spring 1996 Issue

* This work was supported by the Department of Energy contract DE-AC03-76SF00515.

ICFA INSTRUMENTATION BULLETIN

The publication of the ICFA Instrumentation Bulletin is an activity of the Panel on Future Innovation and Development of ICFA (International Committee for Future Accelerators). The Bulletin reports on research and progress in the field of instrumentation with emphasis on application in the field of high energy physics. It encourages issues of the generic instrumentation.

Publisher: Stanford Linear Accelerator Center, SLAC Publications Department, Stanford, CA 94309, U.S.A.

Editor: J. Va'vra
Web Technical Advisers : J. Schwiening and T. Pavel

Cover: The illustration depicts L. J. Waghenaer's marine atlas, "The Mariner's mirror", published in 1588. Lucas Janszoon Waghenaer was born in Holland in the 1530s. He became a famous ship pilot in his time. In 1584, he published the atlas ("Spieghel der Zeevaerdt"), which was greatly valued among mariners for centuries. This was not due only to the map content, but also to the detailed knowledge of navigation techniques of that time. The atlas, as it appears on our page, is the same one used for the Dutch to English translation.

EDITORIAL COMMENT

The ICFA Instrumentation Bulletin is intended to be a forum for people interested in generic instrumentation. The articles should be short, typically a few pages long, and describe either a novel technique or a previously unpublished measurement. We also intend to provide a forum for speculative ideas and not yet proven concepts. We invite articles from industry that describe novel instrumentation techniques. We especially encourage students to try to publish in this Bulletin and hope that their professors will be supportive. However, we discourage "system" descriptions, or papers describing lengthy analysis or software concepts. We believe that such work is already supported by a number of other periodicals and conferences.

What is instrumentation? It is a link between an idea and practical implementation. Although the idea can be formed in front of a blackboard by a theoretical physicist, the instrumentation must be performed in the lab. Good instrumentation work is almost like playing a violin well. If you do not practice, you get out of shape. After a while you tend to "do the instrumentation only in the meetings. " I believe that our forefathers of high energy physics were very good in the lab. In fact, modern physics started with bench top experiments. As experiments grew in size, the software analysis became more complex. People became "virtuosos" in software. The lab work, respective to regular practice on the violin, became technical support. I think the field should recognize that the lab work is as equally important as a good B-meson analysis. If this Bulletin will help this process, I will consider it a success.

It was only after lengthy consideration that I accepted this formidable task. Why should this Bulletin exist? One can easily think: "I do not have time and I will publish in NIM anyway." It is clear that the only way to compete with NIM is to publish fast. It takes up to a year to publish in NIM. The only way to solve this is to bring in some new ideas. Obviously, the new idea is the Web. In principle, it will allow very rapid publication of a paper, almost as soon as it is digested at the editor's end. In addition, we plan to have a **"question-answer"** page which would allow more responsive dialog compared to publishing elsewhere. When five to six articles have been posted on the Web, we will publish the Bulletin.

Web publishing has some drawbacks. Presently, one finds it excessively slow when used at home or when transferring files overseas. Therefore, it is essential that individual articles should be short and must be recallable individually rather than by the whole issue (3-4 minutes per transfer is about maximum one can tolerate). Our Web site is designed such that individual articles can be easily downloaded. A "help" page is available with information on various publishing formats as well as instructions on how to submit an article.

Last but not least, I also wanted to simplify the work at my end and after a discussion with the Bulletin's Web advisers, we decided that articles should be submitted in **paper form** and electronically **(LaTeX** files with **postscript** figures, or a diskette using **MS Word).** The Web format for the published articles will be **postscript (PS) and portable document format (PDF).** We require authors to submit a brief **abstract** enabling the reader to get a short overview of the article.

Jaroslav (Jerry) Va'vra

Please send contributions to:

Stanford Linear Accelerator Center,
Bin 62,
P.O. Box 4349,
Stanford, CA 94309, U.S.A.
e-mail: JJV@slac.stanford.edu

Table of Contents

DEVELOPMENT OF MICROSTRIP GAS CHAMBERS FOR RADIATION DETECTION AND TRACKING AT HIGH RATES FINAL STATUS REPORT

Presented by F. Sauli at the LHCC open meeting, March 13, 1996*

1. INTRODUCTION

Micro-Strip Gas Chambers (MSGCs) have attracted a lot of interest since their introduction by A. Oed [1] due to many promising features: good position accuracy and two-track resolution, high rate capability and low cost. However, medium and long-term stability problems have been met at high radiation rates attributed to substrate charging up and modifications, and ageing due to gas polymerization. To co-ordinate the research on MSGC by various groups, many of them working on tracking devices for the LHC experiments, a proposal for research on micro-strip gas chambers was submitted to the DRDC and approved by the Research Board as RD-28 on June 30, 1992. After three years of collaboration, we can consider the generic R&D on MSGCs to be essentially completed; various groups are however continuing their development in the specific environment and with the constraints of the experiments or applications making use of the new detectors. The full length of the Status Report with a full list of collaborating physicists, institutions and all references can be found in Ref. 2.

2. THE MICRO-STRIP GAS CHAMBER

The basic micro-strip gas chamber (Fig. 1) consists of alternating thin metal strips, anodes and cathodes, typically 10 and 100 μm wide respectively, laid on an insulating support at a distance (pitch) of a few hundred microns. An upper drift electrode, at negative potential, delimits the sensitive gas volume where electrons are released by ionizing radiation. The back side of the support plate can also have a field-defining electrode; in some cases (for very thin substrates) the back-plane can be segmented in readout strips for two-dimensional localization. In the case of low resistivity substrates, the back plane electrode has no effect on the operation of the chamber and can be suppressed. Applying proper potentials to the electrodes, an electric field builds up such that electrons released in the drift space are collected and multiplied when reaching the anodes.

MSGCs have very promising features:

- proportional gains over 10^4;
- position accuracy for x-rays and perpendicular minimum ionizing particles of the order of 30 μm rms ;
- rate capabilities above $10^6\,mm^{-2}s^{-1}$;
- energy resolutions (10.7% FWHM for 5.9 keV X-rays).

Some stability problems were however met from the very beginning: gain modifications due to substrate polarization and charging up, and permanent deterioration (ageing) during sustained irradiation. The physical parameters used in manufacturing and to operate the detectors (substrate material, metal of strips, gas mixture and purity) appear to play a dominant role in determining the long-term stability of operation of the devices; the situation is complicated by the interdependence of the various parameters.

3. CHOICE OF THE SUBSTRATE AND HIGH RATE OPERATION

The choice of the substrate material is crucial to obtain a stable operation of the detector. The major properties to be considered are:

- Good surface quality and metal adhesion properties;
- Excellent surface rigidity to hold high voltage gradients;

- Moderate surface or bulk resistivity to limit surface charging up processes;

Small support thickness and density to reduce multiple scattering and photon conversions, particularly in view of their use as tracking detectors for particle physics experiments;

- Long-term stability of performances in harsh operating conditions;

- Low cost and high reliability, particularly important parameters in view of a massive use in tracking detectors, embedded in set-ups with very limited accessibility.

Most commercially available insulators with good surface quality have a very high resistivity, above $10^{16}\Omega$ cm and an ionic type conductivity; it has been found by many groups that this results in operating 'instabilities of the MSGCs immediately after power on and during irradiation. These effects are attributed to the modification of the electric field by substrate polarization following the application of the potentials on electrodes, and to charging up of the insulator between strips due to the accumulation of electrons and ions, produced in the avalanches, on the surface of the support.

The initial decrease of gain at power on and the bizarre field-dependent behavior of the rate capability, first reported by the CERN group, have been confirmed by the NIKHEF and RAL groups. It is clearly a consequence of polarization effects on the dielectric inducing a time-dependent modification of the field map. While for moderate radiation fluxes use of high resistivity supports can be considered acceptable, and in fact has been adopted for example for the HERMES experiment, the behavior shown can obviously be a source of serious operating instabilities at higher rates.

Another, longer term modification of gain in MSGCs made on boro-silicate glass and exposed to high radiation fluxes has been reported: during sustained irradiation with X-ray sources realized to study the ageing properties of the chambers, a local decrease of gain is observed, recovering however with time towards the original after removal of the source. One should keep in mind that this long-term, recoverable gain modification overlaps to and can be confused with the permanent ageing due the formation of polymers in the gas; it can only be identified in runs realized in very clean conditions, analyzing the gain behavior after stopping the irradiation.

It is generally recognized and experimentally demonstrated that the use of a substrate with lower resistivity and electronic conductivity eliminates the initial polarization effects and the subsequent surface charging processes up to very high rates; in general one also obtains a more stable operation and a reduced ageing rate, if any. The best results in terms of long-term stability at high rates have been obtained with electron-conducting glass, with bulk resistivity in the range 10^{9} - $10^{12}\Omega$ cm, custom-made (the so-called Moscow glass developed by the BINP (Budker Institute of Nuclear Physics)-Novosibirsk), or commercial (S-8900 by Schott). Recently, the BINP group has reported the successful completion of the development of large size, thin electron conducting glass suitable for MSGC manufacturing; the first chambers realized on this glass are delivered at CERN for a long-term beam test set-up in the framework of the CMS tracking group development. The IP (Institute of physics)-Prague group has also developed electron-conducting glass and studied its morphological and electrical properties; Fig. 2 shows an example of measured temperature dependence of the volume resistivity of two types of glass, compared to the commercial Schott S-8900. MSGCs have been built on this glass and successfully operated.

Several methods of conditioning insulating supports to obtain the desired surface resistivity in the range 10^{4}-$10^{15}\Omega$/square have been developed and tested by RD-28 co-operating institutions. In a natural extension of the methods developed in semiconductor industries, several studies of ion implantation or doping by diffusion have been used. The evolution of the gain under continuous irradiation measured with MSGCs manufactured on regular and ion-implanted D-263 glasses shows a much better behavior of the implanted plate;

there is however a small residual gain loss due to charging up or to some other surface-modifying mechanism.

Chemical Vapor Deposition (CVD) of thin diamond-like layers is a well known industrial technology, used both for hardening mechanical components or, more recently, to manufacture ionization detectors. The use of CVD diamond coatings to reduce surface resistivity was suggested long ago by the WIS group (Weizmann Institute of Sciences, Israel), but the standard method appeared not to be able to provide the high values of resistivity required. Recently, the CERN group has found a private research laboratory having this know-how, and able to provide thin coatings in the range 1012-1014 Ω/square. The method (Low Pressure Plasma Assisted Chemical Vapor Deposition, LPCVD) is fast and cheap enough to be a valuable alternative to the use of semi-conducting glass, and allows to coat uniformly a wide range of materials over extended areas. For this particular run, the average value was $1.5 \pm 0.3\, 10^{15}\ \Omega$/square. Diamond coated plates have been extensively tested by the CERN group, and appear to be uniform and stable in the medium term. Large area (100x100 mm^2) MSGCs have been built on diamond-coated glass both with chromium and gold strips, and exhibit excellent rate capabilities as well as ageing properties. Fig. 3 shows the completely flat response of the chambers exposed to high rate x-ray fluxes, up to 2.10^6 counts $mm^{-2}s^{-1}$ at an avalanche size of about 10^5 electrons.

Direct deposition over an insulating support of an electron-conducting glass layer, obtained by sputtering bulk conducting glass, has been developed by the RAL (Rutherford Appleton Lab) group in collaboration with industry. Although promising results have been obtained in terms of rate capability and ageing properties of MSGCs manufactured on plates coated by S-8900 glass, the method has provided so far a fair uniformity of resistivity over extended areas, a known limitation of fixed-target sputtering. However, due to the moderate dependence of gain on surface resistivity, MSGCs manufactured on sputtered glass exhibit an acceptable gain uniformity and energy resolution; the rate capability is largely enhanced, a characteristic of the electron-conducting supports. The ageing behavior is also improved; work is in progress to improve the manufacturing by using larger area or mobile sputtering targets.

Other technologies for surface resistivity control by thin-layer coating have been explored. The LPI (Lebedev Physical Institute)-Moscow group has reported results obtained with ion-beam sputtering of semi-conducting glass and amorphous hydrogenated silicon, as well as low pressure chemical vapor deposition (LP CVD) of amorphous hydrogenated carbon. One characteristic property of some layers is a variation of the bulk resistivity with the electric field; the effect of this behavior on the operation of the detectors remains to be investigated. Moreover, a strong dependence of the resistivity from the light conditions has been observed, particularly for the amorphous silicon layers, another feature requiring thorough investigation.

Over-coating, covering an existing MSGC structure with a thin resistive layer, has also been tried by several groups. Intrinsically simpler, since it avoids possible adhesion problems that can be met when manufacturing the chamber, the acceptance of an over-coat solution depends however on the long-term stability of the thin layer, that acts as interface between the gas and the electrodes and can be damaged by the electron and ion currents, as well as by the reactivity of the various molecular species present in the avalanche. Promising results have been reported by the TRIUMF group using several metals, sputtered in argon over standard MSGCs made on Kapton. As already reported in previous studies, the best results have been obtained with nickel; although evolving with time, the value of resistivity appears to stabilize after a month or so from fabrication. The rate capability of chambers over-coated (or passivated, in the author's language) is excellent demonstrating that in the short term the presence of the layer above (as against below) the conductors has a similar role in preventing surface charging up. In several long-term irradiation exposures, the group has demonstrated also stability of operation up to large collected charges. Less promising results have been reported by the CERN group, observing a systematic degradation of all over-coated structures tested so far when subjected to long-term irradiation.

Continuing its work on advanced thin-film coating technologies, the INFN-Legnaro group has developed a new deposition method to prepare polyimide over- or under-coatings in order to reduce the surface resistivity. Using a vapor deposition polymerization, the group has been able to produce thin polymer layers of accurately controlled thickness; uniformity within a few percent over 80 mm has been demonstrated. The method has been used to realize the passivation of the ends of strips in a MSGC, in order to prevent the well known problem of discharges.

4. MSGC OPERATION

Operating parameters and features of MSGCs such as gas gain, space and energy resolution, signal characteristics, noise and discharge rate have been studied by varying gas mixtures, working potentials, geometrical parameters like the gap, pitch, width of the electrodes, support thickness and potential of the back electrode (if present). In general, the best results in terms of gain and stability of operation have been obtained using mixtures of argon-DME, neon-DME and CO_2-DME in comparable percentages, or pure DME. Other gases used within the collaboration include mixtures with CF_4, a gas known to prevent or even cure ageing processes in multi-wire chambers; some doubts persist however on the effects in the long term of the etching properties of CF_4, as well on the production of electro-negative long lived free radicals in the avalanches.

In an extended study that included, aside from the experimental measurements, also the development of a model for the appearance of discharges, the CERN and BINP groups have analyzed the optimum geometry of MSGC allowing to reach high stable gains. Fig. 4 shows a set of gain curves measured with MSGC plates having identical geometry (7 μm anodes and 200 μm pitch), and different cathode strip widths; an optimum seems to be reached for a width close to 90 μm, a "filling" ratio (metal to insulator) of around 50%. A detailed study of the single electron noise spectra close to the maximum gain seems to confirm the hypothesis that discharges are triggered by an increase in the number of avalanches initiated by electrons released at the cathode edge by ion bombardment or field effect. In view of the strong dependence of the electron emission probability on the electric field and on the work function of the metal used for cathodes, one would expect a large variation in the maximum gain safely reached depending on the manufacturing technology (affecting the detailed shape of the edges) and perhaps the nature of the electrodes. Indeed, maximum gains reached in practice vary from less than a thousand to more than 10^4; the comparison is however often difficult because of the tendency by various groups to only quote relative gain values. Fig. 5 shows a comparative set of absolute gain measurements in different gas mixtures, recently realized by the WIS group in a search for non-flammable alternatives to the most popular choices.

A critical test for the quality of MSGCs is their behavior in presence of heavily ionizing radiation, such as the one generated by neutron-induced reactions at LHC. Recoil protons or activation gamma can easily release in the gas several hundred keV, as against the few keV produced by minimum ionizing particles. The CERN-BINP-MSU groups have observed that in presence of heavily ionizing tracks (et particles from an ^{241}Am source) the maximum safe operating gain is reduced. The CERN-BINP groups have started a systematic investigation on the maximum gain attainable in MSGCs made with chromium and gold strips on electron-conducting substrates and with various operating gases.

The dependence of gain on temperature, another factor affecting the stability of operation, has been studied by the CRN-Strasbourg group. The variation is small, and can be attributed to the change in the gas density. For detectors manufactured on conductive substrates, a change in resistivity with temperature induces another element of variation; as most electron conducting glasses have a negative temperature coefficient, one would expect (equal being the operating voltage) the gain to decrease with temperature, an opposite trend from the one due to the gas itself.

Various other studies have been reported concerning the effect on MSGC substrate and metals of high radiation levels, The CRN-Strasbourg group has systematically investigated the effect of radiation in boro-silicate glass analyzing the density of radiation-induced defects in the bulk with the Electronic Para-Magnetic Resonance method.

The UC-London-RAL groups have studied the effect of neutron irradiation on MSGC, both experimentally and theoretically. Exposing a MSGC made on S-8900 glass to an intense neutron beam at the ISIS spallation facility at RAL, the authors have measured the induced energy spectra and compared with Monte-Carlo simulations. A more extensive work estimating the contribution of the major neutron-induced reactions has been presented at the Lyon workshop and suggests a considerable contribution to background noise of the various processes; the choice of materials for MSGC manufacturing, of the strip's metal and of operating gas may play a critical role in the background levels, and should be thoroughly investigated by the LHC groups.

Several alternatives are possible for the metal used for the strips, depending on the manufacturing technology: aluminum, chromium and gold are the most common choices. Various arguments have been proposed in favor or against each choice, such as the conductor resistivity and the long-term ageing behavior; the final choice depends on the expected operating conditions and on cost considerations. The CERN-BINP group has investigated in detail the properties of MSGCs made with chromium, a good choice in terms of the excellent quality of the photolithography and low costs, but limited to relatively short strip lengths due to signal attenuation, and possibly more sensitive to ageing in presence of pollution ,

5. AGEING

Ageing, or fast degradation of the performance of the detectors during irradiation, is the most serious problem encountered with MSGCs and has been extensively studied experimentally. Permanent damage of the plates has been associated with the production in the avalanches of polymeric compounds, sticking to the electrodes or to the insulator, and perturbing the counting action and inducing discharges. MSGCs have been found to be particularly prone to ageing, possibly because of the small effective area used for charge multiplication; some gases (hydrocarbons) induce very fast ageing, while others like dimethylether (DME) and carbon tetra fluoride (CF_4) allow extended lifetimes.

A careful selection of the operating gas and materials used in manufacturing appears mandatory to guarantee survival of the devices in a high radiation environment. A systematic study of outgassing properties of various materials considered as construction elements for chambers has been performed with the CERN RD-10 set-up, which includes an X-ray long-term irradiation facility and gas monitoring system (a combined mass spectrometer-gas chromatography). The set-up allows to make long-term exposures to radiation with continuous monitoring of currents, pulse heights and physical conditions both in the test chamber and in a monitor counter; materials under test can be an integral part of the chamber construction, or introduced in a "reaction" box in the gas line. Similar set-ups for studying long-term operation of detectors under sustained irradiation have been built at LIP-Coinbra and LPPE-Mons.

A systematic investigation of ageing under sustained irradiation has been performed by several groups within the collaboration using MSGC plates manufactured on various substrates and operating conditions. In optimal laboratory conditions, a long-term survival without degradation up to a collected charge above 100 $mC\,cm^{-1}$ has been demonstrated, corresponding (at an avalanche size of $2{\cdot}10^5$ electrons) to a radiation dose for minimum ionizing particles of 10 MRad, or more than 10 years of LHC operation at maximum luminosity. One example is provided in Fig. 6, obtained with a chamber made with chromium strips on electron-conducting glass, and using as construction materials those recommended by previous outgassing studies.

The majority of ageing tests is realized, for practical reasons, exposing the detector to a high intensity X-ray flux, and accelerating the experiment taking as normalization factor the total collected charge per unit length of strips. It has been found however by the CERN group that, at

least when using boro-silicate glass supports, use of excessively large radiation rates (current densities) results in an optimistic estimate of the ageing rate. This is illustrated in Fig. 7, result of a set of measurements realized in different positions on the same plate at several values of flux. While no gain modifications appear at high current densities, substantial ageing is seen at the lower values. While the exact mechanism of this behavior is not clear, the observation invalidates some previous measurements realized at excessive current densities and casts a general doubt on the adequacy of accelerated ageing tests. Based on this observation, the group recommends to use, for the systematic tests, current densities not exceeding 10 $nA\,mm^{-2}$, an acceleration factor of 20 compared to LHC rates; a final verification at rates closer to real would however seem mandatory.

It appears that, together with the purity of the gas system, dominant factors in determining ageing rate are the nature of the support and the metal used for the strips; the strength of the drift field also seems to play a role. The NIKHEF group, using D-263 glass, has observed a clear improvement replacing aluminum with copper, gold and nickel for the strips. It is suspected that long-term modifications or charging-up of the boro-silicate glass play a role in explaining the observed behavior. This is confirmed by the observed recovery from "ageing"; one could speculate that the different ageing rates for different metal could be due, at least in part, to the different surface conditions of the plates, an outcome of the manufacturing process. The dominant role of a moderate surface resistivity in determining the gain stability is demonstrated by measurements realized by the same group on a MSGC manufactured on D-263 sputtered with S-8900 electron conducting glass, showing a much better performance up to several $mC\,cm^{-1}$.

The RAL group has also systematically investigated the role of metals and supports on the ageing rates. The large difference in ageing rate was measured on two MSGCs manufactured in aluminum and gold on electron-conducting glass. The same group has recently reported the good ageing properties of detectors made on boro-silicate glass, sputtered with a thin layer of low resistivity S-8900 glass; gold strips behave considerably better than aluminum and allow to reach the 100 mC cm^{-1} benchmark with a moderate 10% gain loss .

Measurements realized by the CERN group on chambers manufactured on diamond coated glass have also confirmed the dominant role of the low substrate resistivity in determining ageing behavior. A detector made with chromium strips and irradiated at moderate current density (9 nA mm^{-2}) could reach 80 mC cm^{-1} without gain deterioration . It should be noted that the measurement was realized with a standard gas system set-up, without the strict cleanliness requirements of the dedicated laboratory of the same group.

6. RD-28 MAJOR ACHIEVEMENTS AND CONCLUSIONS

In the three years since the approval of the RD-28 project, the collaboration has expanded from the original number of 40 proponents to 170 physicists and engineers from 40 institutions. A large number and variety of prototype MSGCs have been manufactured and successfully tested in the laboratory and in beams; some have been incorporated in experiments and have already contributed to the improvement of the results. It has been demonstrated that a reasonably good operation at moderate rates can be obtained with supports made on commercially available boro-silicate glass, such as D263, that can be obtained in a wide range of thicknesses, and confirmed that intrinsically more stable operation can be obtained with chambers made on slightly conductive supports. The development of special electron-conducting thin glass, with bulk conductivity in the range 10^{9} to $10^{12}\,\Omega$ cm, and of various surface conditioning methods to reduce resistivity to around $10^{15}\,\Omega$/square has been successfully completed; a new technology for diamond-like coating seems to be particularly successful.

The conditions necessary to guarantee the lifetime of the detectors at high radiation rates suitable for the LHC experiments have been determined, with integral collected charges in accelerated laboratory tests exceeding 100 mC cm^{-1}, equivalent to ten years of operation in

vertex detectors at LHC. The major role of using low resistivity substrates in reducing the ageing rate has been established.

The operating characteristics of the MSGCs have been experimentally measured and predicted using computer simulations, developed to better understand some properties of the detectors and allow the optimization of their design.

Basic manufacturing techniques have been investigated and tested in view of establishing the criteria for a cost effective large scale production; while gold remains the best choice material for the strips, due to its low resistivity and better resistance to ageing, the alternative choice of chromium (an intrinsically cheaper and better known technology) has undergone careful investigations to clarify the size limitations due to the resistivity of the metal, and the possible enhancement of ageing processes.

Various readout schemes and highly integrated electronics circuits, originally developed for solid state detectors to be used at LHC, have been tested, both at the basic level and on detectors operating in realistic conditions; analysis of the data aimed at improving the time resolution has suggested the best strategy for bunch crossing identification.

Special devices have been successfully developed, such as thin plastic MSGCs for transition radiation detectors, plates with non-parallel (keystone) geometry, very thin layer detectors for two-dimensional readout, photon-sensitive and scintillating chambers. Charge multiplication with MSGCs in liquid xenon has been demonstrated.

Micro-strip gas chambers are now integral constituents of several present and future detectors, such as HERMES and CMS; the teams involved in the basic research are now integral part of those experiments.

The members of the RD-28 collaboration consider the generic research on micro-strip gas chambers to be successfully completed, and do not request therefore a continuation of the project. The present is therefore the final status report of the RD-28 collaboration.

REFERENCES

[1] A. Oed, Position -Sensitive Detector With Micro-strip Anode for Electron Multiplication with Gases. Nucl. Instr.& Methods **A263** (1988) 351.

[2] F. Sauli, RD-28 Status Report: CERN/LHCC 96-18, LDRB Status Report/RD-28, February 14, 1996.

* The Status Report was condensed for the purposes of the ICFA Bulletin by the editor.

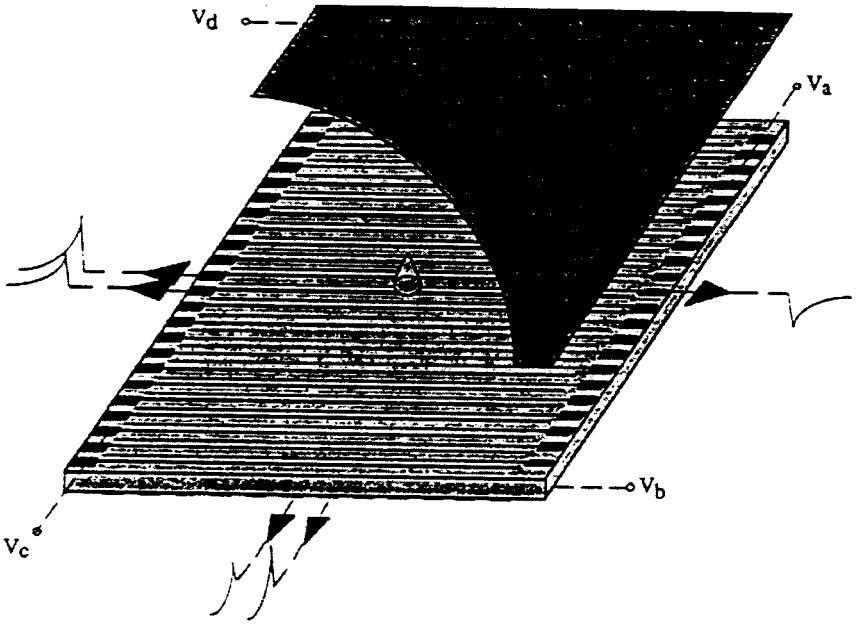

Fig. 1: Schematics of a MSGC and of the signals induced by an avalanche.

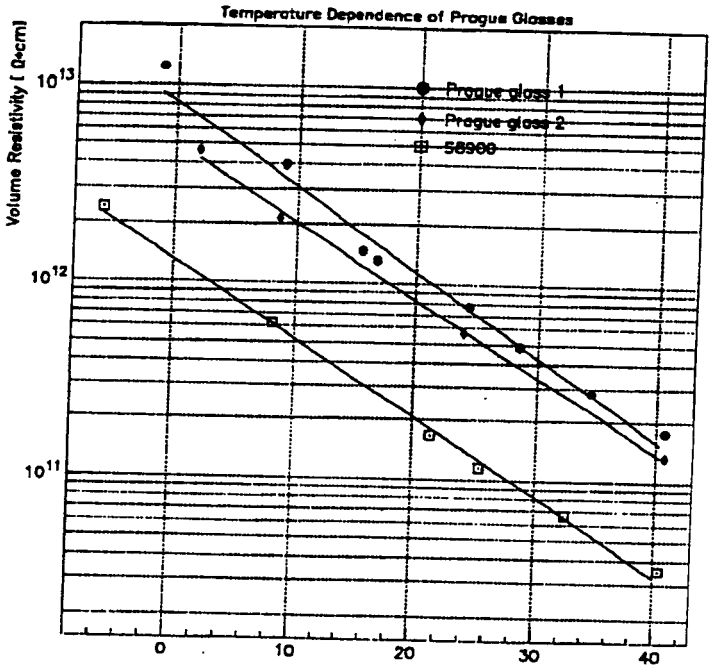

Fig. 2: Temperature dependence of resistivity in several electron-conducting glasses.

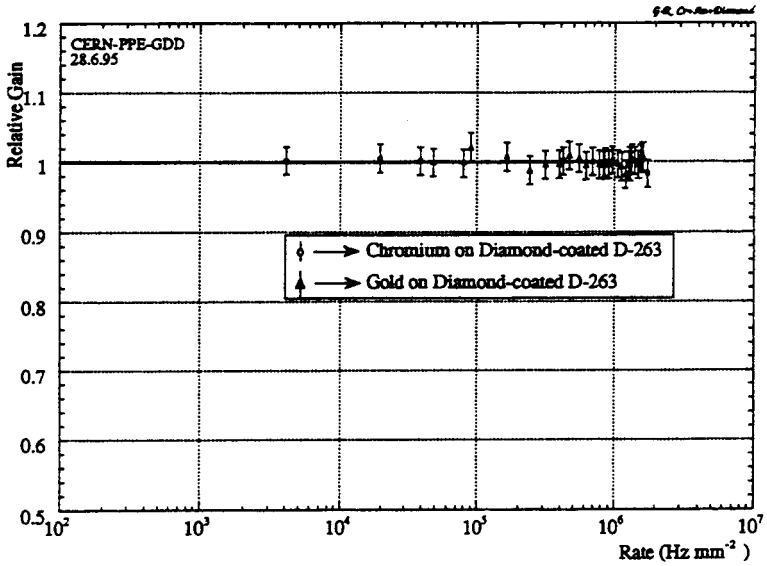

Fig. 3 : Rate dependence of gain for MSGCs made with chromium and gold on diamond-coated glass.

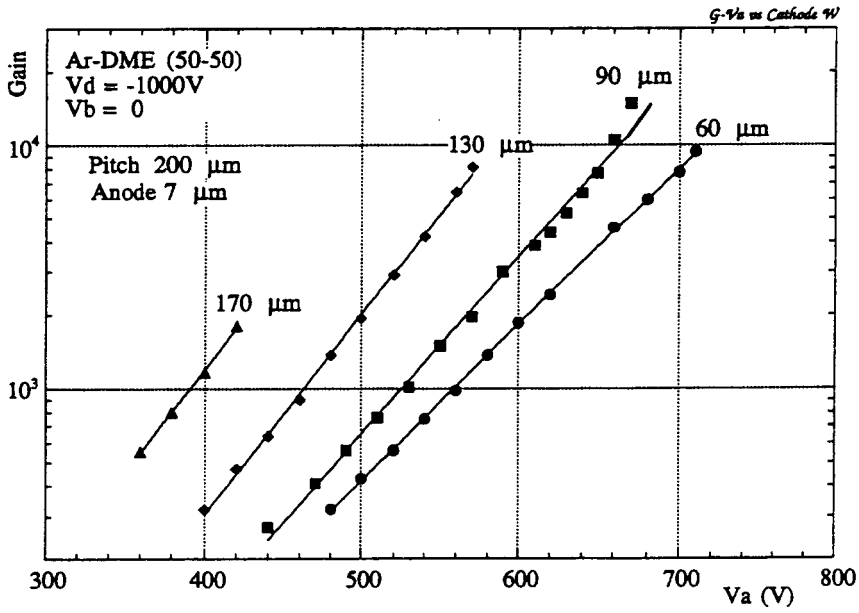

Fig. 4 : Maximum gain reachable in MSGCs having equal anode widths and pitch, for different cathode widths.

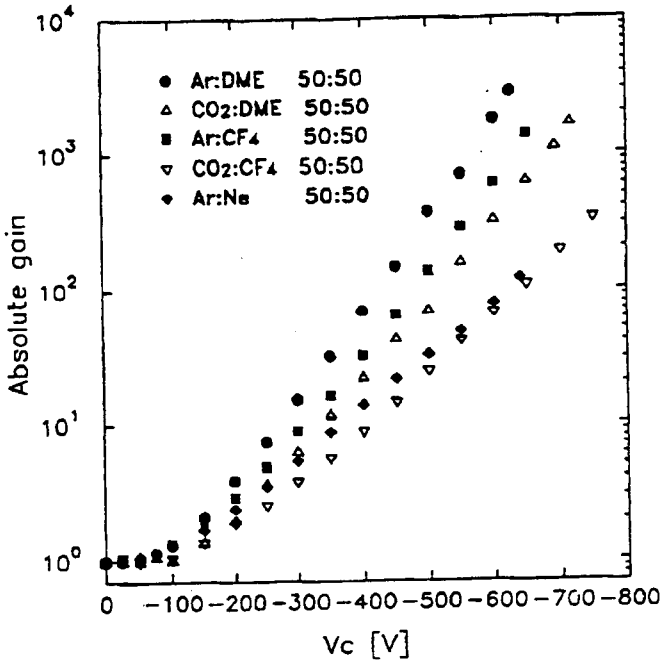

Fig 5: Absolute gain vs. voltage measured for several gas measured in a standard 200 μm pitch MSgC.

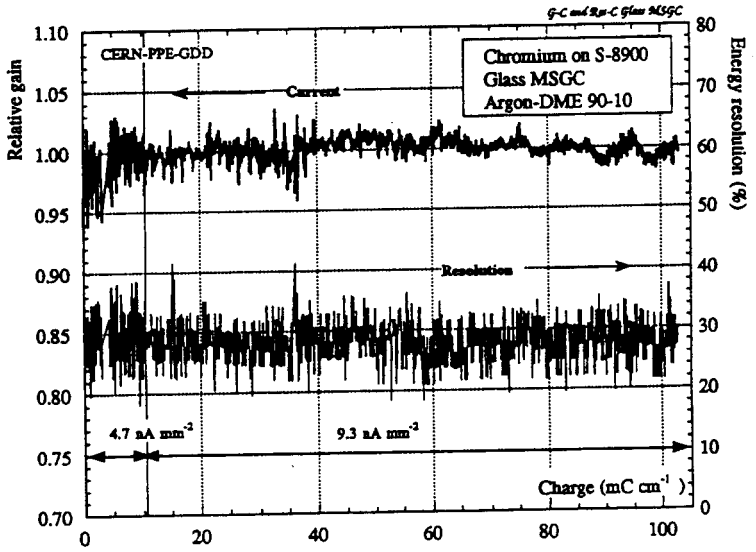

Fig. 6 : Long term ageing test: gain and energy resolution as a function of collected charge. Chromium MSGC on electron-conducting glass.

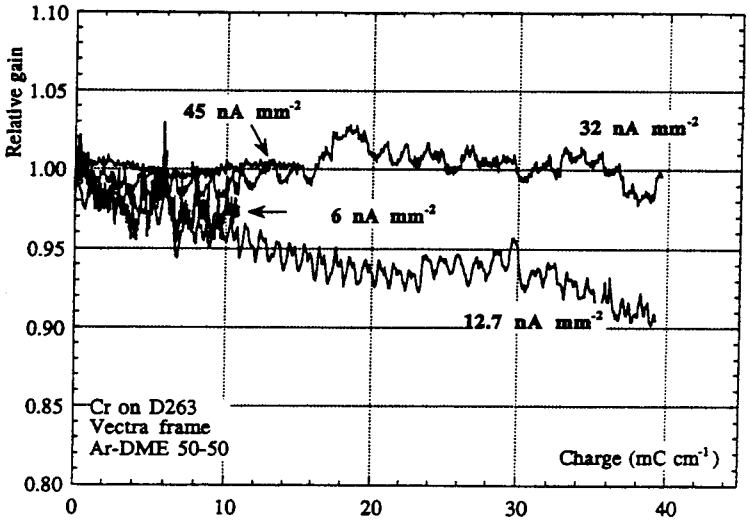

Fig. 7: Current density (dose rate) dependence ageing measurements. Chromium strips on D-263 glass.

This page intentionally left blank.

March 18, 1996

THE MULTIGAP RESISTIVE PLATE CHAMBER

E. Cerron Zeballos[1,2], I. Crotty[1], D. Hatzifotiadou[1,2], J. Lamas Valverde[1,2,3], S. Neupane[1,2], M.C.S. Williams[1] and A. Zichichi[4]

1) LAA project, CERN, Geneva, Switzerland
2) World Laboratory, Lausanne, Switzerland
3) University Louis Pasteur, Strasbourg, France
4) University of Bologna and INFN, Bologna, Italy

ABSTRACT

This paper describes the multigap resistive plate chamber (RPC). This is a variant of the wide gap RPC. However it has much improved time resolution, while keeping all the other advantages of the wide gap RPC design.

1. INTRODUCTION

The goal of current R&D on Resistive Plate Chambers (RPC) is to produce a low cost detector that has good timing, space resolution sufficient for trigger purposes (readout strips of several cm width) and can withstand a flux of several kHz/cm^2 (i.e. a device for the muon trigger at LHC). Two types of RPCs can be considered as candidates. The more conventional RPC with a 2 mm gas gap was initially developed to operate in streamer mode at very low flux. However it has been shown that one can operate it with a high fraction of freon (e.g. 85% freon 13B1) in avalanche mode. Another approach is to have a wide gap RPC and operate it in avalanche mode with more conventional freon-free gas mixtures. We have discussed the relative differences in performance previously [1]. One finds a smaller dynamic range of gain for the wide gap, thus one can operate it with a lower average avalanche charge for a given threshold. This leads to a higher rate capability and lower power dissipation in the gas volume; however it is easier to get good timing with narrow gap RPC. In this paper we discuss a new development of the RPC: the multigap RPC. We show that with this detector one can keep the advantages of the wide gap RPC, but have substantially improved timing. We also found other significant advantages with the multigap design which results in a longer efficiency plateau and better rate capability; the reasons for this enhanced performance will be discussed in a subsequent paper.

2. THE REASON FOR THE MULTI-GAP

In a parallel plate chamber, the gas gap is used both for the creation of the primary ionization clusters and also for the gas gain. The signal generated is by avalanche multiplication across the gap. The number of electrons, N, in an avalanche is given by: $N=N_o e^{\alpha x}$, where α is the first Townsend coefficient, x the distance the avalanche has progressed from its initial position and N_o the initial number of electrons. Thus the generated signal depends on the position of the primary ionization clusters. With conventional non-flammable gas mixtures used in gaseous detectors, the number of primary ionization clusters is 3-4 clusters/mm. Primary ionization follows Poisson statistics; thus to work at efficiencies close to 100%, a detectable avalanche signal needs to be produced from a single electron cluster located anywhere within the closest 1-1.5 mm to the cathode. This has been previously discussed in our paper concerning the wide gap RPC [2]. The variation in the position of the initial clusters of primary ionization generates a time jitter. Typically, at the electric fields usual in the wide gap RPC, the drift speed of electrons is ~10 ns/mm; thus we would expect time resolutions with a full width at base (FWAB) in the order of 15 ns. This is what we observe [1]. The 2 mm gap RPC has been operated in avalanche mode with a high fraction of Freon 13B1 by us [1] and other researchers in this field [3,4]. Since Freon 13B1 is heavy, the number of primary ionization clusters should be ~10 clusters/mm. Thus

variations in the position of primary ionization within the first 300-400 μm will define the time resolution. It is no surprise that the 2 mm gap chamber has a better time resolution.

Our goal is to improve the time resolution of the wide gap RPC without undue sacrifice of its other good qualities. The principle advantage is the lower dynamic range of signal; this leads to smaller current flowing through the gas gap and resistive plates. This allows operation at a higher rate and also lower power dissipated in the gas gap. Another advantage is that the larger gap is less sensitive to unavoidable variations of the gap width; thus mass production of large areas becomes easier.

One way around this problem of the distribution of primary ionization over 1.5 mm (i.e. the cause of the large time jitter) is to divide up this 1.5 mm into smaller slices. For example in figure 1 we show (schematically) a 9 mm gap divided into 3 x 3 mm gaps. The voltage is still applied on electrodes mounted on the outside surfaces of the chamber. The internal plates are electrically floating, taking a voltage due to electrostatics. On average each sub-gap produces a detectable avalanche for a through-going minimum ionizing particle, but the limiting case is when just one sub-gap generates a detectable avalanche. In this limiting case the initial cluster of primary ionization is within 0.5 mm of one of the three cathode surfaces; thus one could expect a threefold reduction in time jitter.

Obviously it is necessary to operate these two devices with a different Townsend coefficient, α. For example, we consider an RPC with one 9 mm gap filled with a gas that produces an average of 3 primary ionization clusters per mm for a minimum ionizing particle. 99% of through-going charged particles produce ionization within the 1.5 mm closest to the cathode. If we set the gas gain to be 10^6 over the remaining 7.5 mm, then a single electron avalanching over this distance would produce a signal of 10 fC (only 7% of the total charge generates the fast signal due to the movement of the electrons). This 10 fC signal appears to be a reasonable lower limit for the threshold for electronics in use today on large area detectors. The gas gain of a single electron avalanching over the full 9 mm would be $1.6\ 10^7$. We refer to this ratio of gain as the 'dynamic range of gain' (=16 in this case). In order to have this gas gain, the value of the Townsend coefficient has to be $\alpha/p = 0.024$. In the case of 3 x 3 mm gas gaps, 99% of through-going charged particles produce ionization within any of 0.5 mm regions closest to the cathode plate of all sub-gaps (as shown in figure 1). The minimum signal is when only one gap has a detectable avalanche, with a single electron avalanching over 2.5 mm. Since the avalanche forms over a factor 3 shorter distance, the induced signal is a factor 3 smaller; thus to produce a 10 fC signal we need an avalanche that generates $3\ 10^6$ electrons. An electron that avalanches over the full 3 mm would produce an avalanche of $5.9\ 10^7$ electrons. In this case the dynamic range of gain is 20 (similar to the value of 16 obtained for the 9 mm mono-gap), but we need to operate with an α/p of 0.078. In general α/p increases exponentially with electric field [5]; thus a higher α/p implies also a larger $d\alpha/dE$. Sharma and Sauli [5] were unable to measure values of α/p much above 0.04 due to the onset of spark breakdown in their test cell. Thus we find that this triple-gap chamber has a similar dynamic range of gain to the 9 mm mono-gap, but a much increased Townsend coefficient. Our concern was that for such a high value of the Townsend coefficient, it may be difficult to find a gas that gives a long stable efficiency plateau. However, as the results of section 4 show, a suitable gas can be found.

The two LHC experiments, ATLAS and CMS, propose using double-gap RPCs in 'OR' [6,7]. Is the principle of operation of these double-gap RPCs different from the multigap RPCs described in this paper? Obviously the multigap allows a greater number of sub-gaps; we are now building a 6 gap version (3 sub-gaps on each side of a read out strip board in a similar manner to the device proposed for LHC). We have also built a multigap RPC consisting of 2 x 4 mm gas gaps. In a comparison with the 3 x 3 mm multigap, one would expect the 2 x 4 mm chamber to have a degraded time resolution, but maybe an improved efficiency plateau (since one works at a lower Townsend coefficient) and also an improved rate capability (since there is one less resistive plate in the chamber). However the 3 x 3 mm has a longer efficiency plateau, especially at high fluxes. This suggests these intermediate plates have an unexpected beneficial effect on the performance of the chamber.

Some reasons are suggested in section 5; obviously a more in-depth study is needed. In addition the proposed RPCs for LHC use a 2 mm gap; thus unavoidable gap variations have a much larger effect than the 9 mm triple-gap design discussed here.

3. CONSTRUCTION OF THE MULTI-GAP RPC

We use a similar construction technique as for our more standard wide-gap RPCs. The outer resistive plates are made from melamine-phenolic foils 0.8 mm thick. The surface facing the gas is melamine; the electrodes are fixed to the phenolic surfaces. The intermediate dividing plates are melamine-phenolic-melamine foils 0.8 mm thick. A printed-circuit board with strips forms the anode; the strips are on a 15 mm pitch with 0.25 mm inter-strip gaps. This is glued to the melamine-phenolic resistive plate with an epoxy* with a volume resistivity, $\rho = 10^{11\text{-}13}\ \Omega$ cm. The cathode is a pad of conductive nickel paint (1 $\Omega/\square$). The intermediate plates were held in place with spacer bars 6 mm wide and 3 mm in height. These spacer bars run the length of the chamber with a small gap at the end to allow for gas flow. These spacer bars and the wider (3 cm wide) bar that made the frame around the edge of the chamber were glued to the melamine surfaces with double-sided tape. The glue layer of this tape has a thickness of 100 μm. When the chamber had been fully assembled we potted the outside edges with dilute CAF-4#; this made the chamber gas-tight and reduced any corona from the edge of the melamine sheets. These spacer bars were offset from layer to layer so that any through-going particle would only miss one layer due to spacers. The active area of the chamber is 24 x 24 cm^2.

4. TEST BEAM RESULTS

This chamber was tested in the T9 test beam in the East-hall at CERN. The polarity of the final quadruple was reversed in order to defocus the beam so that the whole active area of the chamber was exposed to a uniform flux (i.e. flood illumination). The total length of the spill was 400 ms with a 250 ms flat top. The electronics used was similar to the electronics used for our previous RPC tests [8]. The threshold is ~10 fC and peaking time 5 ns. The efficiency versus voltage is shown in figure 2; we also show the dark current. The gas mixture used was 86% Argon, 8.5% CO_2, 0.5% C_4F_{10} and 5% DME. We did not obtain a good efficiency plateau for gas mixtures without the addition of 0.5% C_4F_{10}. We have worked with C_4F_{10} previously (with a single wide gap chamber) [8], obtaining a better plateau but losing in rate capability. Previously, we had also found that the shape of the plateau changed with rate. For the multigap chamber, we see no change in plateau shape, just an overall reduction of efficiency at the highest rate. The rate capability is more than equal to the best of the wide gap chambers [1].

The time spectra of the average of the leading and trailing edge of the signal (similar to what one would expect from a constant fraction discriminator) is shown in figure 3 for an applied voltage of 16 kV (200 V above the knee of the efficiency plateau). The charge spectrum of the fast signal is shown in figure 4, also for a voltage of 16 kV.

5. DISCUSSION

We have tested a new type of RPC: the multigap RPC. Basically we have taken a conventional wide-gap RPC and added some inner resistive plates to divide the wide-gap into sub-gaps. In this example, we have tested a 3 x 3 mm gap RPC. One worry is that these inner resistive plates are electrically floating; how can we ensure that they take the voltages as shown in figure 1? We could add some electrode within the frame and apply a voltage to these inner resistive plates (around the edge of the chamber); however we do not think that this is necessary. The reason is that these inner resistive plates are in a strong electric field and therefore take a voltage due to electrostatics. If for any reason the voltage on one plate

---

* CY1311-HY1300, Ciba-Geigy Araldite Electronics Resins, Ciba-Geigy Plastics, Duxford, Cambridge, England.

Rhodorsil CAF-4 (Usine Silicones B.P. 22, 69191 Saint-Fons Cedex) diluted with cellulose thinners.

deviates, this will cause an increase of electric field in one sub-gap and a decrease in the other; the gap with the higher field will produce larger avalanches (i.e. more charge) compared to the other sub-gap producing smaller avalanches. We see that this will restore the voltage to its proper value so as to equalize the field in the two sub-gaps. We have now tested this chamber with a variety of gases and rates and find the behavior consistently good. We therefore suspect that leaving these inner plates electrically floating is a stable solution. Obviously we will test larger chambers to verify this concept.

The multigap technique allows us to add many internal spacers, thus we can arrange to have through-going particles passing through a maximum of one spacer. Also since the spacer has a higher relative dielectric constant ($\varepsilon \sim 4$) than gas, the electrostatic coupling between the avalanche (in the remaining sub-gaps) and the pick-up strips is enhanced. This will help alleviate any reduction in efficiency around a spacer. However it should be noted that these internal spacer bars will help eliminate the need for external large flat plates, originally thought necessary for constructional purposes.

We can build a multigap RPC on either side of a pick-up strip board (similar in concept to those proposed for the CMS experiment). Thus the timing will further improve and the efficiency plateau extend to lower voltages. We intend to test this concept. The only disadvantage (compared to the conventional wide-gap RPC) is an increase of the strip multiplicity. Indeed we observe an increase, but it is small (the average increases from 1.5 to 2 strips per cluster). Since we suspect that some of our cluster size is caused by cross-talk within the pre-amplifiers mounted on the chamber, we avoid giving a precise number until we have studied this problem in more detail.

One problem with the conventional RPC is that extra large avalanches charge a local spot on the surface which results in local inefficiency. If these internal plates are thin enough, a local deposition of charge on a surface of one of these will indeed cause a local decrease in electric field (and thus efficiency) in one sub-gap, but the neighboring sub-gap will have an increase in field. This compensation helps to produce a longer efficiency plateau. It should be noted that all these internal resistive plates have electrons from avalanches fed into one side, and positive ions into the other. On average there should be no net flow of charge into or out of these plates.

6. CONCLUSION

Our initial tests of a new type of RPC are extremely promising. The time resolution is equal to the best we have obtained with the 2 mm gap chamber (operating in pure avalanche mode). The rate capability is equal to the best we ever managed with a conventional wide-gap RPC. In addition the dark current is very low and the efficiency plateau long and stable. Recently we have discovered that avalanche fluctuations play a key role in the understanding of the benefit of the multigap; this will be addressed in a future paper.

ACKNOWLEDGEMENT

In all our work we are indebted to the service of the PS division, which provides such a useful facility of test beams in the CERN East hall. In addition, we have had to parasite on the beam allocation to other groups in order to test this chamber. We thank everyone that has helped make this such a pleasant possibility.

REFERENCES

1. A comparison of the wide gap and narrow gap Resistive Plate Chamber. E. Cerron Zeballos, I. Crotty, D. Hatzifotiadou, J. Lamas Valverde, S. Neupane, V. Peskov, S. Singh, M.C.S. Williams and A. Zichichi, CERN PPE/95-146, CERN/LAA-MC 95-21 and submitted to Nucl. Instr. and Meth.
2. The Wide Gap Resistive Plate Chamber, I. Crotty, E. Cerron Zeballos, J. Lamas Valverde, D. Hatzifotiadou, M.C.S. Williams and A. Zichichi, Nucl. Instr. and Meth. A 360(1995)512.
3. R. Cardarelli, A. Di Ciaccio, R. Santonico, Nucl. Instr. and Meth. A333(1993)399.
4. C. Bacci et al. Nucl. Instr. and Meth. A352(1995)552.
5. See for example: A. Sharma and F. Sauli, Nucl. Instr. and Meth. A 334(1993)420.

6. ATLAS Technical Proposal, CERN/LHCC/94-43, LHCC/P2, Dec. 15, 1994.
7. The CMS Technical Proposal, CERN/LHCC 94-38, LHCC/P1, Dec. 15, 1994.
8. Latest Results of the Wide Gap RPC, E. Cerron Zeballos, I. Crotty, D. Hatzifotiadou, J. Lamas Valverde, S. Neupane, V. Peskov, S. Singh, M.C.S. Williams and A. Zichichi, presented at the 3rd International Workshop on Resistive Plate Chambers and Related Detectors, Pavia, Italy. 11-12 Oct. 1995.
9. E. Cerron Zeballos et al., Nucl. Instr. and Meth. A 367(1995)388.

FIGURE CAPTIONS

1. Schematic diagram and principle of operation of multi-gap RPC compared to a conventional 9 mm single gap RPC.
2. Efficiency versus high voltage for various fluxes. The beam was defocused, thus the whole active area of the chamber exposed. The gas mixture was 86% Argon, 8.5% CO_2, 0.5% C_4F_{10} and 5% DME.
3. Time spectra of the average of the leading and trailing edge timing at 16 kV (200 V above the knee of the efficiency plateau).
4. Charge spectrum of the fast signal taken at 16 kV (200 V above the knee of the efficiency plateau).

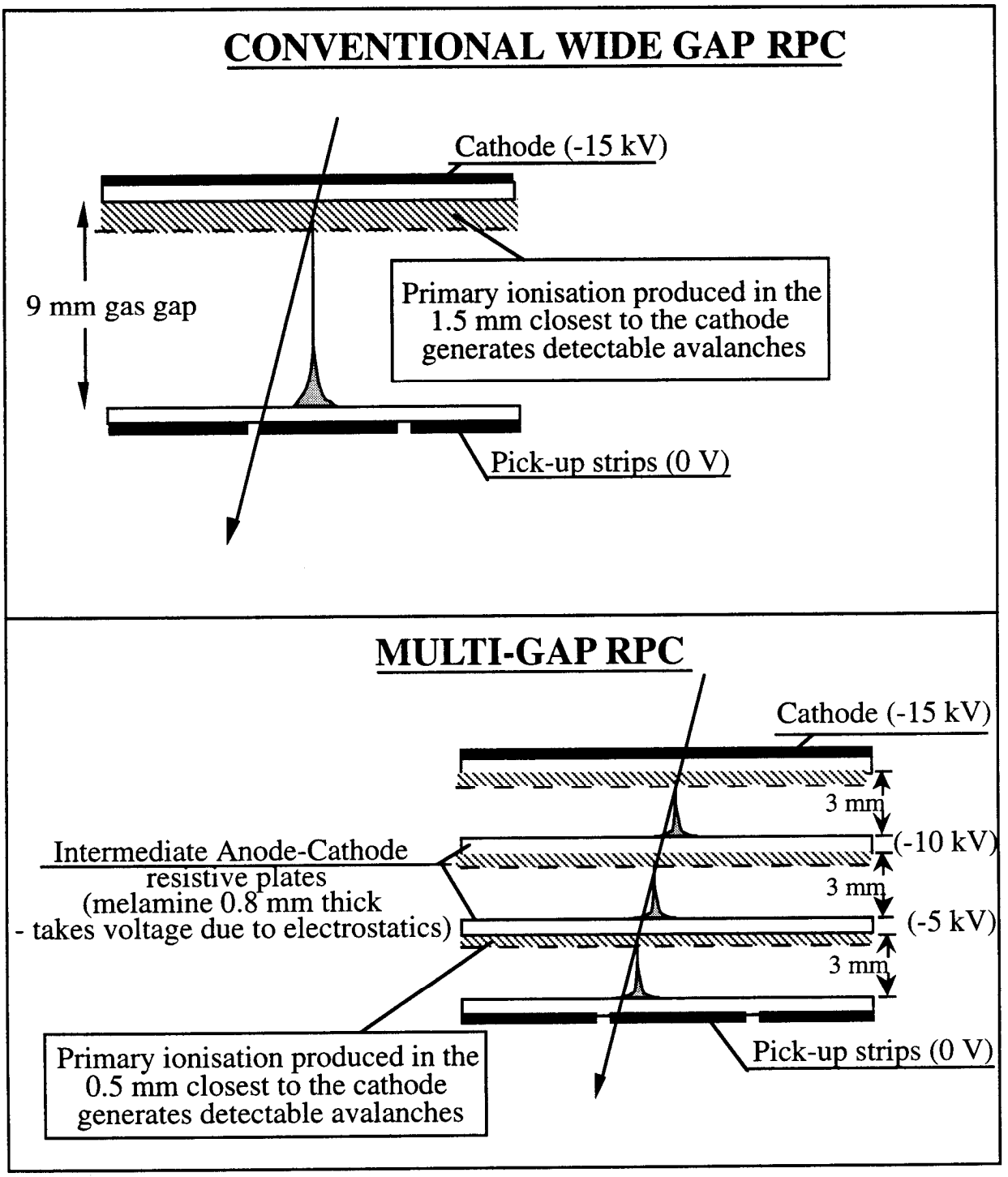

Figure 1

Schematic diagram and principle of operation of multi-gap RPC compared to a conventional 9 mm single gap RPC.

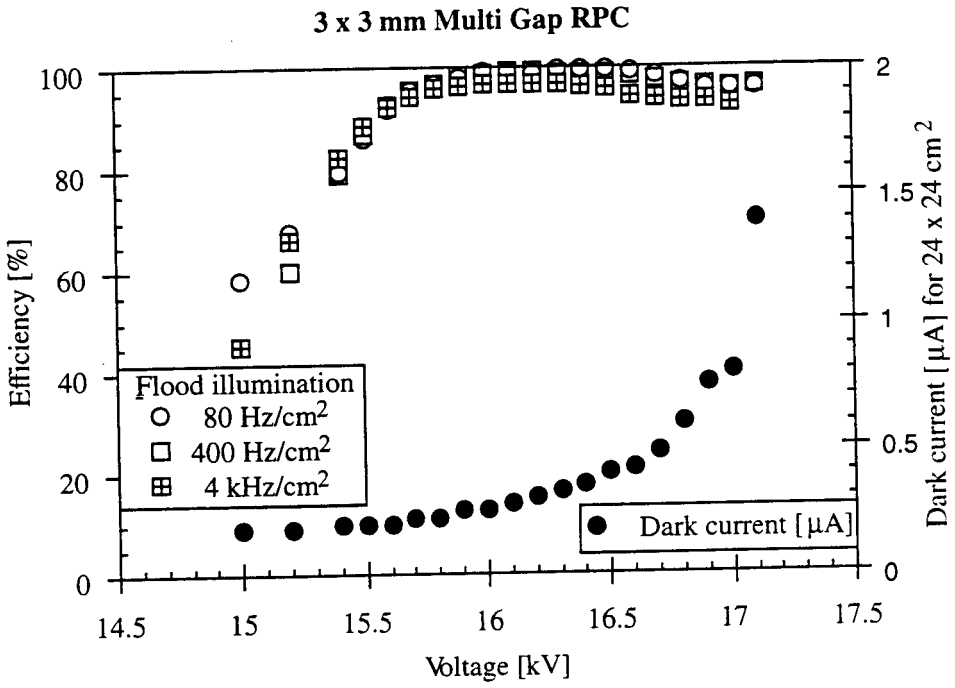

Figure 2

Efficiency versus high voltage for various fluxes. The beam was defocused, thus the whole active area of the chamber exposed. The gas mixture was 86% Argon, 8.5% CO_2, 0.5% C_4F_{10} and 5% DME.

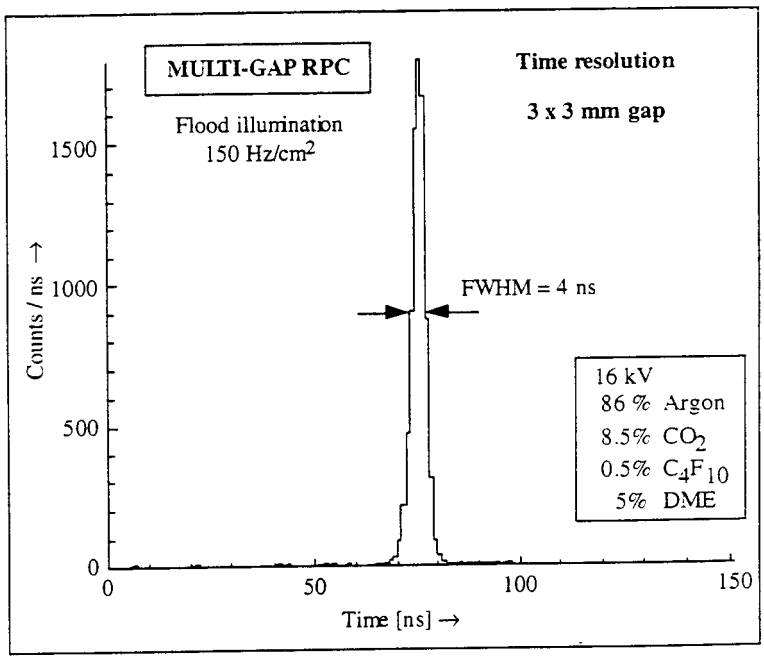

Figure 3

Time spectra of the average of the leading and trailing edge timing at 16 kV (200 V above the knee of the efficiency plateau).

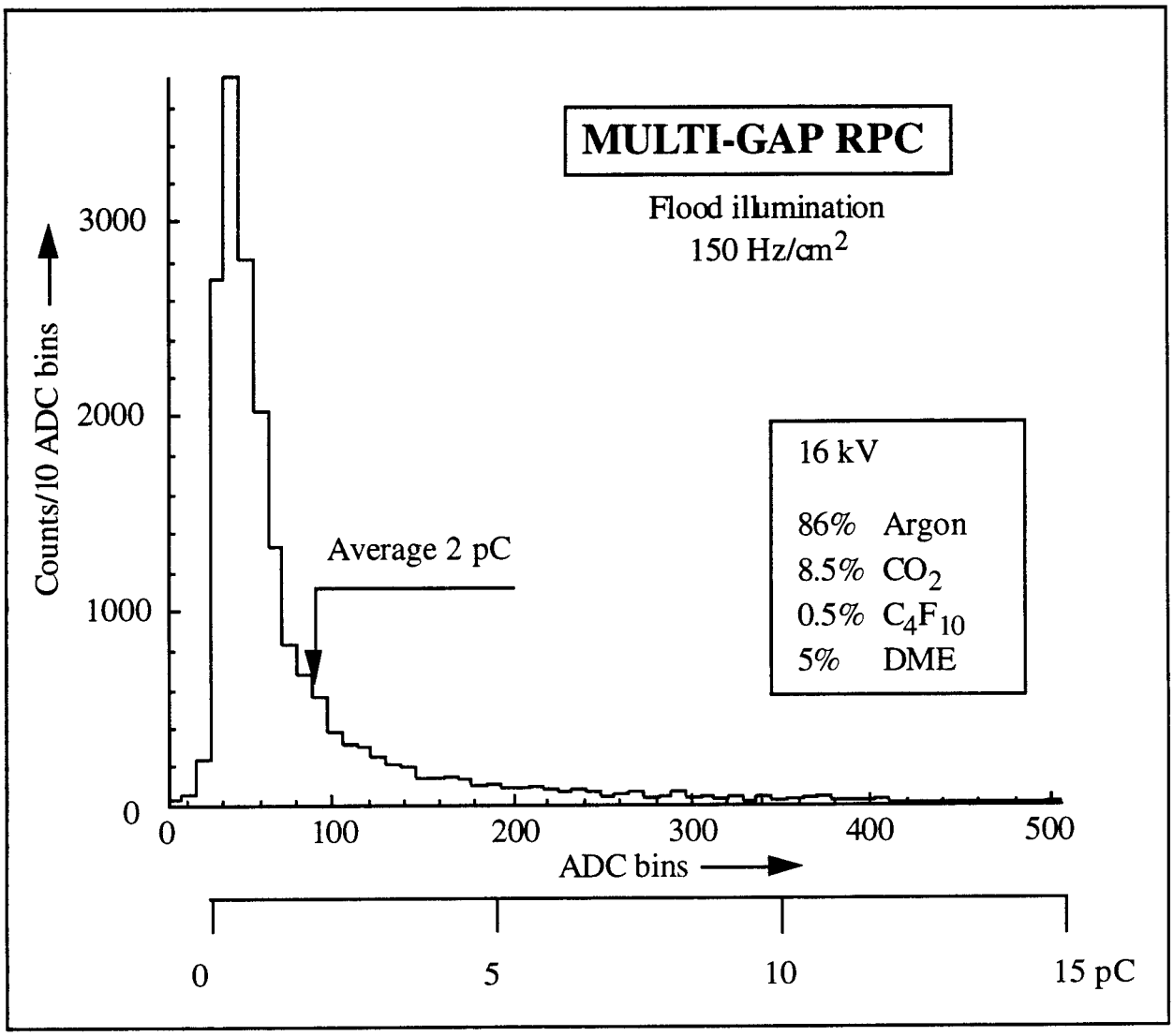

Figure 4

Charge spectrum of the fast signal taken at 16 kV (200 V above the knee of the efficiency plateau).

SOLID AND VAPOUR PHASE UV PHOTOCATHODES FOR GASEOUS DETECTORS

G. Vasileiadis, G. Malamud*, Ph. Miné and D. Vartsky†

LPNHE, Ecole Polytechnique, IN2P3-CNRS,
91128 Palaiseau, France

ABSTRACT

We measured the relative quantum efficiency of four organic materials: tetrathiafulvalene and bis(cyclopentadienyl) magnesium in the solid phase and t-butylferrocene and n-butylferrocene in the vapour phase. The measurements were performed in the wavelength range of 150-220 nm. We also present a new quantum efficiency measurement of ethylferrocene. The three ferrocene derivatives exhibit relatively high quantum efficiency.

1 Introduction

Large area photosensitive gaseous wire chambers can provide a cheap and unique solution for fast and high accuracy localisation of UV photons emitted by Cherenkov radiation or by scintillator. As a photocathodes, in the vapour phase, TMAE (tetrakis[dimethylamine] ethylene) is used in a large number of experiments operating in high-energy physics, astrophysics, and nuclear medical imaging [1,2]. In the solid phase, cesium iodide is the most popular candidate envisaged in future RICH devices [3,4]. The vapour phase photocathode presents several advantages: the light absorption length can be controlled by the gas flow and the temperature, the photosensitive material is constantly renewed and thus does not suffer from aging. On the other hand the use of

*Presently at CERN, Geneve, Switzerland.

†Presently at Soreq Nuclear Research Center, Yavne, Israel.

a solid photocathodes is favorable for fast timing and parallax-free imaging, as all photoelectrons are emitted from a well-defined surface. Devices based on this principle do not require complex temperature regulation of the gas system of the detectors.

An important drawback of the photocathodes is its reactivity to oxygen and to other materials. TMAE is difficult to handle from this point of view, and a great deal of effort has been devoted in recent years to search for compounds which exhibit a comparable quantum efficiency (QE) and are easier to handle[5]. CsI has received a lot of attention because it can be handled for a reasonable time in air[6]. The QE of CsI is however lower than that of TMAE by more than a factor 2 for wavelengths higher than 190 nm[7].

In this article we will present for the first time a measurement of the QE of four organic materials, known for their low ionization potential : TTF(tetrathiafulvalene) [8], bis(cyclopentadienyl) magnesium $(C_5H_5)_2Mg$, t-butylferrocene $(CH_3)_3CC_5H_4Fe(C_5H_5)$ and n-butylferrocene $(C_4H_9C_5H_4)$-$Fe(C_5H_5)$. The last three belong to a family of metallocenes to which the attention was drawn by Anderson [9]. We also present a new measurement of the QE for ethylferrocene $C_2H_5C_5H_4FeC_5H_5$.

Several authors [10,7,11] reported that the standards used for light flux calibration, for absolute QE measurements may be unreliable. We have been confronted with this problem following a recalibration of our reference photomultipliers (Hamamatsu R1460) [7]. As a consequence of this recalibration the absolute value of TMAE QE as measured by us is a factor of 2 larger then the widely accepted value of Holroyd et al. [12]. The problems encountered in absolute determination of QE will be presented in a separate communication[13]. We express therefore our present results in a relative form by comparing them to the results obtained from the measurements on TMAE and CsI. To avoid any problem of calibration when comparing solids and vapours in this study, the results of the compounds in the solid and vapour phase are compared to those of CsI and TMAE respectively.

2 Bis(cyclopentadin) Magnesium, TTF

Since both these compounds are in powder form, (STREM Chem. Inc. and Aldrich-Chimie-SARL, respectively), the samples were prepared by vacuum deposition of a thin layer on a copper disk. The samples were stored under argon atmosphere. A small exposure to air, of about 5 rein, was necessary during the transport to the measuring apparatus.

For the first compound, Bis(cyclopentadin) magnesium, a sample with a 500nm thickness was measured both in vacuum and in methane. In both cases no measurable signal was detected.

The second compound, tetrathiafulvalene (TTF), was measured only in vacuum. Two samples

of different thickness, 300nm and 500nm, were studied. No influence of thickness was observed. The results, relative to the QE of CsI obtained from these measurements are shown in figure 1. The detected signal was weak in both cases, resulting in a low QE throughout the whole spectral range.

3 Ferrocene

As was mentioned earlier, three sets of measurements were performed with Ferrocene compounds. Two of these materials, namely the ethylferroce and the t-butylferroce are air-stable liquids, while the third one, n-butylferrocene, is not. All three compounds were purchased from STREM Chem. Inc. The procedures of measuring the QE of these liquids is described in detail in [14]. In addition, different gas flow and temperature schemes were used to ensure that there were no systematic errors during the measurements.

Figure 2 shows the results obtained for ethylferrocene vapour normalised to TMAE measurements. In addition the curve that corresponds to an indirect measurement performed by Charpak et al. [15] is shown in dashed line. For comparison purposes it is normalised to TMAE QE as measured by Holroyd et al. [12]. The two other curves correspond to two different gas flows. Both measurements were performed at 20°C. A measurement performed on a sample from a different source [16] exhibited no significant difference in the QE.

The QE measured, in both cases, gave similar results within the experimental errors. The QE reaches at best 30% of that of TMAE. A third measurement at 30°C, not shown here, gave also a similar result. Comparing our data with the one reported in [15], we notice a strong disagreement in the region around 180-190 nm. Our results do not peak, while the latter show a clear increase of the QE. Except from the fact that the curve shown in [15] is based on an indirect measurement of the QE, it should be noted that the measurement was done at 70°C.

Similar measurements were done with the t-butylferrocene (TBF) sample, shown in figure 3. The measured QE is lower than that of EF. The distribution is rather flat, reaching about 15% of the value of TMAE at 150nm followed by a decrease, with a cutoff around 200nm. Again here, the two curves stand for the different gas flow. These measurements were performed at 30°C.

Finally figure 4 shows the results obtained for the n-butylferrocene (NBF) compound. The results obtained at two different flows are markedly different. Different results occurred either when changing the flow of gas or when changing the orientation of the detector from vertical to horizontal position. A possible explanation could be related to the fact that this liquid has a much more viscous form than the previous ones. Taking into account that with our current setup, it is

not possible to raise the temperature of the bubbler to more than 40°C, the uniformity of the gas mixture during the period of the measurement might not be very stable. This could introduce a non-controllable variation of the NBF vapour pressure. We therefore cannot precisely conclude on the QE of NBF. From the two plots of Fig.4 one could estimate that the QE lies within 10% and 20% of the TMAE value, up to 180nm, falling monotonically towards a cutoff around 200nm.

4 Conclusions

Several photosensitive compounds were measured by us in previous works: decamethylferrocene, tris(cyclopentadienyl) cerium [17], 1,1'-dimethylferrocene, bis(cyclopentadienyl) ruthenium and amorphous silicon with different doping levels [18].

Including in our survey the present data of TTF, ethylferrocene, bis(cyclopentadienyl) magnesium, n-butylferrocene and t-butylferrocene, we can draw the following conclusion concerning the QE. Only the derivatives of ferrocene exhibit potentially useful QE values. Similar organometallic compounds, containing different metallic elements, (cerium, ruthenium, magnesium) have much lower QE than those containing iron. Decamethylferrocene has some unique characteristics: it is solid, its QE is non-negligible at 220 nm and it is not air-sensitive. The three liquids, ethylferrocene, n-butylferrocene and t-butylferrocene have a QE in the range 10% to 30% of the TMAE QE between 150 and 190 nm. At larger wavelengths their QE drops abruptly. They could be used in some cases as alternatives to TMAE.

5 Acknowledgements

We would like to thank A. Breskin and R. Chechik of the Weizmann Institute of Science, Rehovot, Israel for constant support and fruitful discussions.

6 Addendum

Question from the editor concerning the Q.E. normalization:

> On page 2, I would conclude that you quote all Q.E. measurements relative to your TMAE measurements, which has twice as high Q.E. **compared to Holroyd?** However on page 3, I read that your denominator is Holroyd's TMAE measurement. As far as the CsI normalization, you used the Breskin/Mine measurement?

Answer from the author (P. Mine):

> The idea is that everything is measured in the same apparatus. We have two procedures, one for vapours (including TMAE), one for solids (including CsI). Thus our new photocathodes are compared either to TMAE or to CsI, depending on their phase. Of course we use the **"Mine** measurement" for CsI, which is found identical to the "Breskin measurement" after several years of common studies. At this level we don't need any data from the rest of the world. A problem comes if we want to put together the vapour and solid measurements: TMAE is too high or CsI is too low, compared to the literature. We discuss this in detail in ref [13], which is written, but not submitted yet. If we believe our absolute standard (PM Hamamatsu R1460 recalibrated versus NIST photodiode [7]) it is our TMAE which is too high **by a factor of 2.** Holroyd's TMAE data is used only when we want to plot the dashed curve on figure 2, i.e. to quote the ethylferrocene measurement published by Charpak et al. [15]. It is the only other experiment I know, concerning the molecules we tested in the present paper.

References

[1] J. Seguinot and T. Ypsilantis *Nucl. Inst. & Meth.,* A343: 1, 1994.

[2] G. Charpak et al. *J. Nucl. Med.,* 15:690, 1989.

[3] E. Nappi, G. Paic, F. Piuz, and R.S. Ribeiro. *Nucl. Inst. & Meth.,* A315:113, 1992.

[4] J. Friese. private communication, Proposal for High Acceptance Di-Electron Spectrometer, GSI, Darmstadt., 1994.

[5] P. Min . *Nucl. Inst. & Meth.,* A343:99, 1994.

[6] V. Dangendorf, A. Breskin, R. Chechik, and H. Schmidt-Böcking. *Nucl. Inst. & Meth.,* A308:519, 1991.

[7] A. Breskin, R. Chechik, D. Vartsky, G. Malamud, and P. Min . *Nucl. Inst. & Meth.,* A343:159, 1994.

[8] R. V. Gemmer et al. *J. Org. Chem.,* 40:3544, 1975.

[9] D.F. Anderson. *IEEE Trans. on Nucl. Sci.,* 28:842, 1981.

[10] P. Besson, P. Bourgeois, P. Garganne, J.P. Robert, L. Giry, and Y. Vitel. *Nucl. Inst. & Meth.,* A344:435, 1994.

[11] P. Dorenbos, J.T.M. de Haas, R. Visser, C.W.E. van Eijk, and R.W. Hollander. *Nucl. Inst. & Meth.,* A325:369, 1993.

[12] R.A. Holroyd, J.M. Preses, C.L. Woody, and R.A. Johnson. *Nucl. Inst. & Meth.,* A261:440, 1987.

[13] G. Vasileiadis, G. Malamud, Ph. Min , D. Vartsky, A. Breskin, and R. Chechik. Problems encountered in the determination of absolute quantum efficiency of UV photocathodes, submitted to Nucl. Instr. & Meth., 1995.

[14] H. Braining, A. Breskin, R. Chechik, P. Min , and D. Vartsky. *Nucl. Inst. & Meth.,* A327:369, 1993.

[15] G. Charpak et al. *Nucl. Inst. & Meth.,* A277:537, 1989.

[16] We thank Prof. Lemenovski (Moscow Univ.) for providing the ethylferrocene sample.

[17] G. Malamud, P. Min , D. Vartsky, B. Equer, P. Besson, P. Bourgeois, A. Breskin, and R. Chechik. *Nucl. Inst. & Meth.,* A348:275, 1994.

[18] G. Malamud, P. Min , D. Vartsky, B. Equer, A. Breskin, and R. Chechik. *Nucl. Inst. & Meth.,* A343:121, 1993.

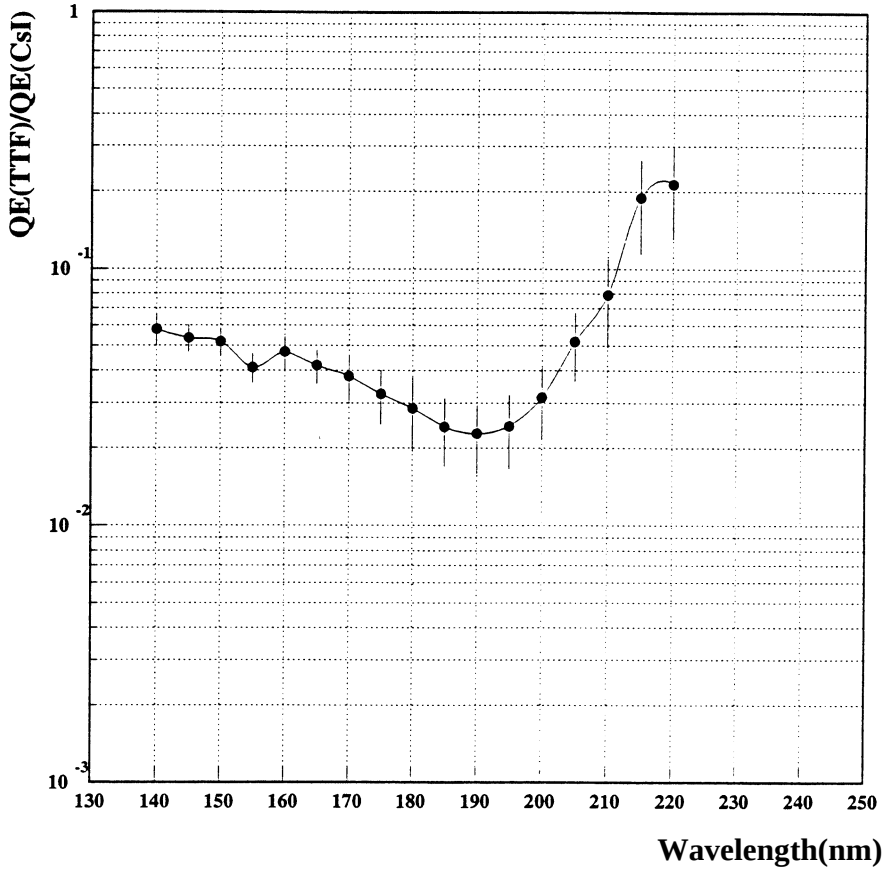

Figure 1:

The Quantum efficiency of tetrathiafulvalene (TTF) relative to CsI.

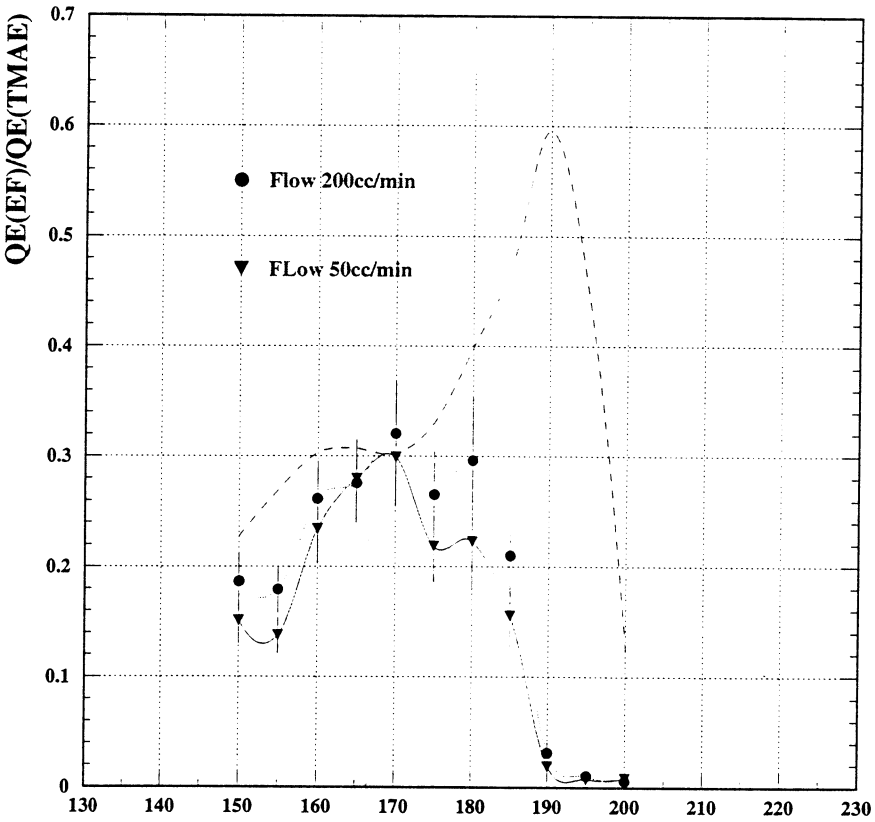

Figure 2:

The Quantum efficiency of ethylferrocene (EF) gas photocathodes relative to TMAE. dashed curve is from [15]. Measurements were made at two different flows of methane atm.

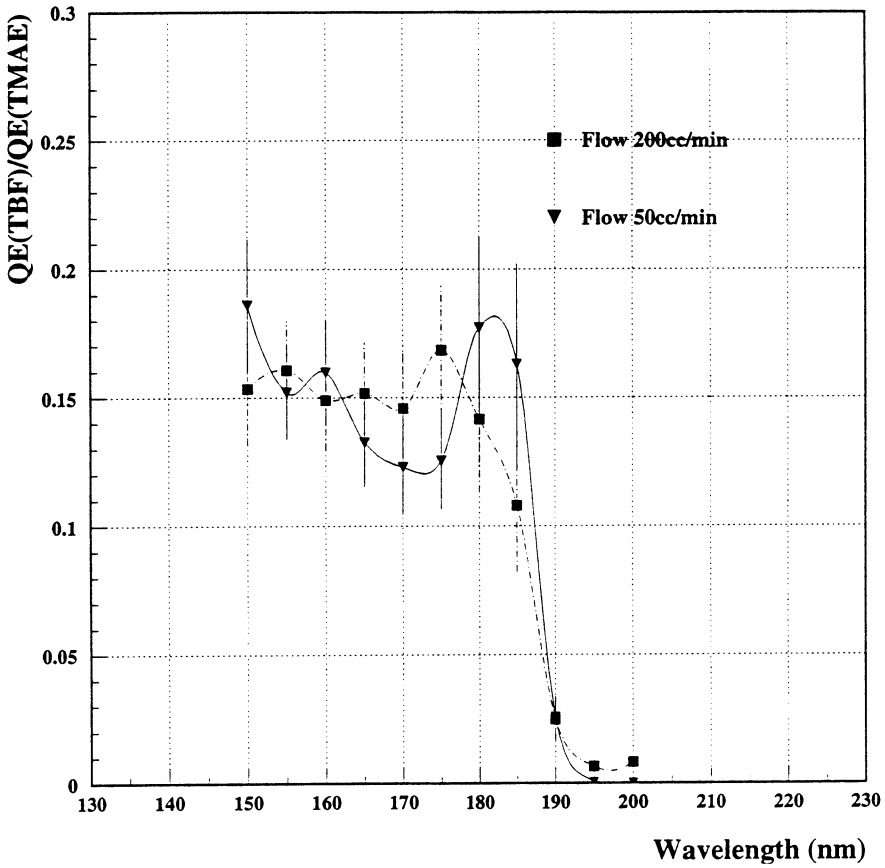

Figure 3:

The Quantum efficiency of t-butylferrocene (TBF) relative to TMAE for two different flows of methane at 1 atm.

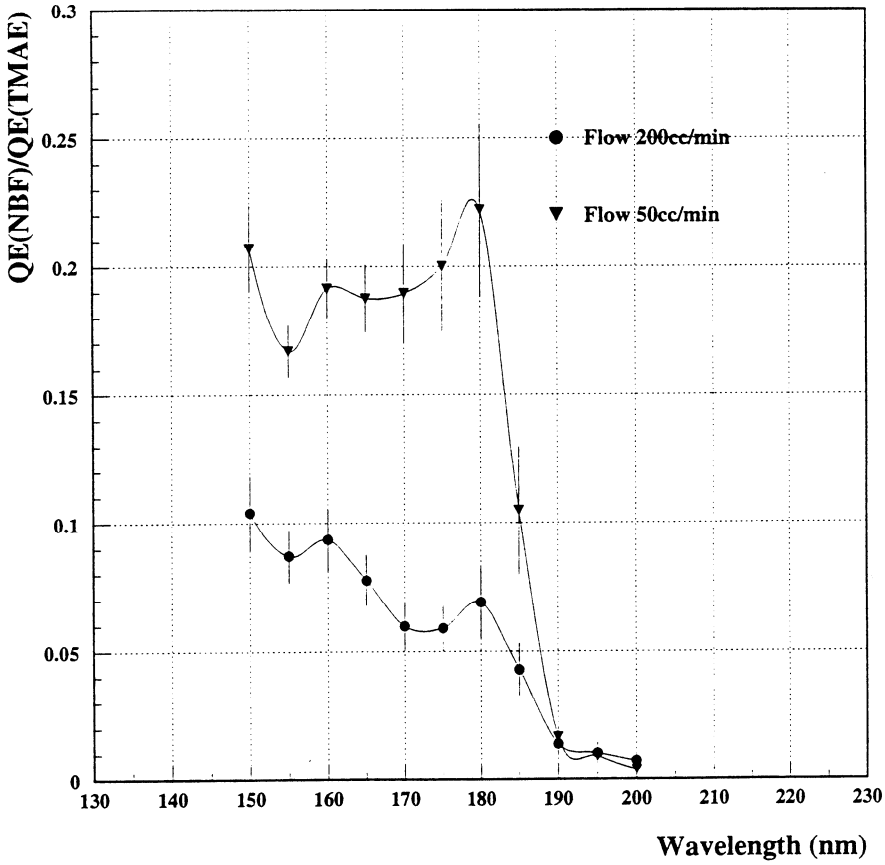

Figure 4:

The Quantum efficiency of n-butylferrocene (NBF) relative to TMAE for two different flows of methane at 1 atm.

TOWARDS GASEOUS DETECTORS FOR VISIBLE PHOTONS

A. Breskin, A. Buzulutskov, R. Chechik, E. Shefer

Department of Particle Physics
The Weizmann Institute of Science, 76100 Rehovot, Israel

ABSTRACT

NaI protective coatings invisible cesium-antimony photocathodes have been studied. Protected photocathodes are shown to withstand exposure to considerable doses of oxygen and dry air. This opens ways to their handling and operation in gaseous detectors for visible photons.

Since the venue of wire chambers, scientists have dreamt to replace vacuum photomultipliers by photosensitive gaseous detectors. Compared to vacuum photomultipliers, such devices can be made very large and should be considerably less sensitive to magnetic fields. Gaseous detectors of photons have been successfully operated so far only in the far ultraviolet (UV) range [1–3]. This progress is due to a large extent to a relative stability of the photosensitive materials in a counting gas and under short exposure to air.

However, no effective photoconvertors above 210 nm has been found, which could withstand contact with even minute amount of oxygen, water and other impurities. In order to operate such devices, it was suggested to protect sensitive photocathodes by their coating with various solid dielectric films [4–6]. However, the few attempts [7,4] to protect visible photocathodes were not successful so far.

In this letter we show for the first time that cesium-antimony (Cs_3Sb) photocathodes, sensitive in the close UV and visible range, can withstand cent act with considerable amount of oxygen and dry air, when coated with thin NaI films. More complete description of the results are presented elsewhere [8].

The experimental setup for preparation and characterization of visible photocathodes consists of a high vacuum (10^{-9} Torr) chamber coupled to a monochromators (Fig. 1). The system permits a displacement of the photocathodes substrate between three positions inside the vacuum chamber:

for the preparation of the photocathodes, the evaporation of the protective film and the measurement of the quantum yield (QY). In the present work the absolute QY was measured in a reflective mode in vacuum. The exposure of the photocathodes to gas was performed inside the chamber at room temperature.

Fig.2 shows the QY drop of a Cs_3Sb photocathodes, coated with a 151 Å thick NaI film, as a function of the residual oxygen pressure inside the chamber; the exposure time at each data point is 5 min. At each wavelength the QY is rather stable up to an oxygen pressure of about 0.1 Torr and then decreases gradually. One should note that an oxygen pressure of 150 Torr (the last pressure point in Fig.2) corresponds approximately to its partial pressure in air. It is important to remark that an uncoated photocathodes was found by us to completely disintegrate already at an oxygen pressure of 10^{-5} Torr.

We compared the protection capability of NaI films with that of CsI (see Fig.3). The protection capability of CsI films was found to be comparable with that of NaI, for an equal post-coating attenuation oft he photoyield and for oxygen pressures below 10^{-2} Torr. However for higher pressures it is appreciably smaller compared to NaI.

We have tried to protect Cs_3Sb photocathodes with other dielectric films, such as CsF, NaF, SiO and hexatriacontane. However the electron transmission of these films was lower and the protection capability was much smaller, compared to that of NaI and CsI. Thus, for the time being NaI can be considered the most successful protective film among those investigated by us.

In conclusion, one can state that the concept of protection of visible photocathodes has been proven [8]. This can open new avenues in light detection techniques. The realization of this concept in the present work resulted in the crest ion of a relatively efficient and air-stable photoconvertor sensitive in the wavelength region of 250-450 nm. This can be regarded as a considerable step forward in this field, since the introduction, more than 15 years ago (see Refs. 1 and 3), of air-stable photosensitive materials in the wavelength region below 220 nm. The search for other protective layers, with better photoelectron transmission and higher protection capability, is being carried out in our laboratory.

References

[1] J. Seguinot and T. Ypsilantis, Nucl. Instr. and Meth. A **343,** 1 (1994), and references therein.

[2] J. Va'vra, Photon detectors. Preprint SLAC-PUB-95-6961, Proc. of the 2nd Int. Workshop on RICH Detectors, June 12-16, 1995, Uppsala, Sweden, Nucl. Instr. and Meth. A, in press, and references therein.

[3] A. Breskin, CsI UV photocathodes: history and mystery. Preprint WIS-95/31/July-PH, Proc. of the 2nd Int. Workshop on RICH Detectors, June 12-16, 1995, Uppsala, Sweden, Nucl. Instr. and Meth. A, in press, and references therein.

[4] V. Peskov, A. Borovik-Romanov, T. Sokolova, E. Silin, Nucl. Instr. and Meth. A **353,** 184 (1994).

[5] A. Breskin, A. Buzulutskov, and R. Chechik, IEEE Trans. Nucl. Sci. **42,** 298 (1995).

[6] A. Buzulutskov, A. Breskin, R. Chechik, and J. Va'vra, Study of photocathodes protection with thin dielectric films, Preprint WIS-95/32/July-PH, Proc. of the 2nd Int. Workshop on RICH Detectors, June 12-16, 1995, Uppsala, Sweden, Nucl. Instr. and Meth. A, in press.

[7] R. Enomoto, T. Sumiyoshi and Y. Fujita, Nucl. Instr. and Meth. A **343,** 117 (1994).

[8] A. Breskin, A. Buzulutskov, R. Chechik, and E. Shefer, Evidence for thin film protection of visible photocathodes, Preprint WIS-96/10/Feb.-PH, submitted to Appl. Phys. Lett.

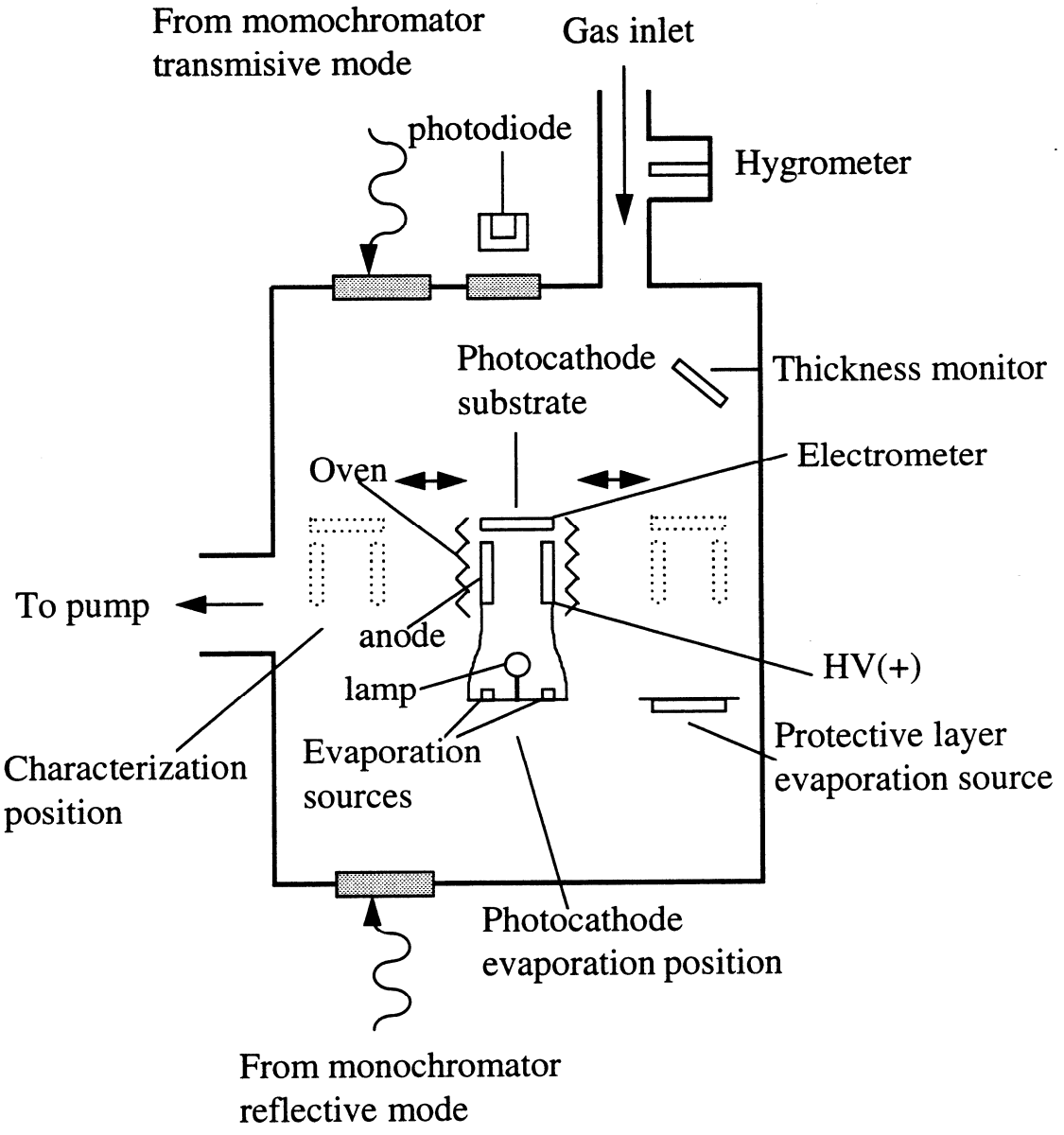

Fig. 1 Experimental setup the preparation of visible photocathodes, evaporation of protective films and their characterization.

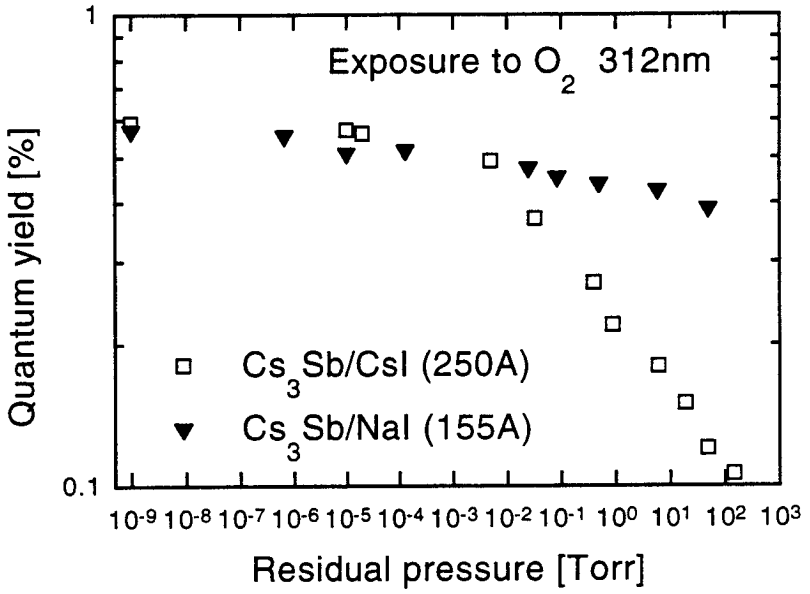

Fig.2 Evolution of a NaI-coated Cs_3Sb photocathodes under exposure to oxygen. Shown are the absolute quantum yield values of a Cs_3Sb photocathodes coated with 151 Å thick NaI film, measured at different wavelengths, as a function of the residual oxygen pressure during the exposure. Exposure time at each data point is 5 min.

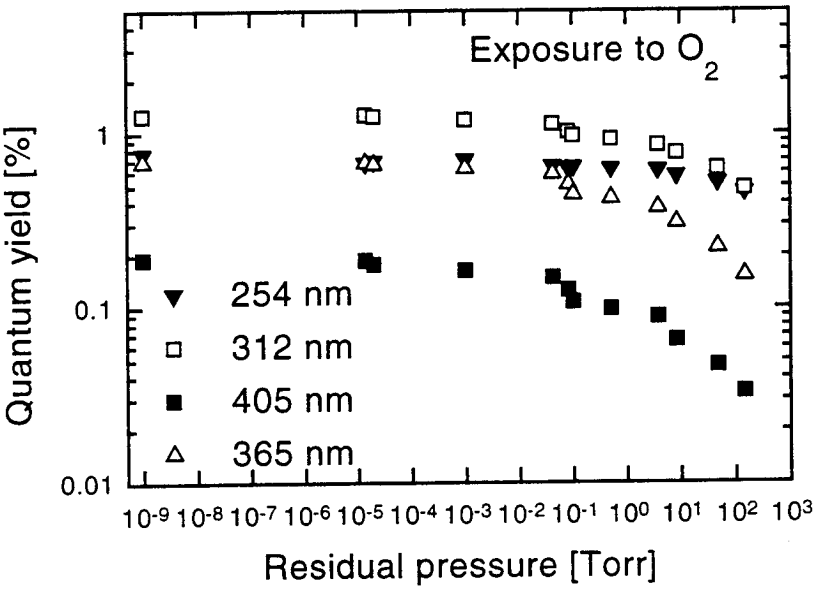

Fig.3 Comparison of the protection capability of NaI and CsI coating films. Shown are the absolute quantum yield values of Cs_3Sb photocathodes coated with 155 Å thick NaI and 250 Å thick CsI films, at 312 nm, as a function of the residual oxygen pressure. Exposure time at each data point is 5 min.

A NEW TECHNIQUE FOR STUDYING THE FANO FACTOR AND THE MEAN ENERGY PER ION PAIR IN COUNTING GASES

A. Pansky, A. Breskin and R. Chechik

Particle Physics Department, The Weizmann Inst. of Science 76100, Rehovot, ISRAEL

ABSTRACT

A new method is presented for deriving the Fano factor and the mean energy per ion pair in the ultrasoft x-ray energy range. It is based on counting electrons deposited by a photon in a low-pressure gas, and is applicable for all counting gases. The energy dependence of these parameters for several hydrocarbons and gas mixtures is presented.

A fundamental topic in radiation physics and dosimetry deals with the number of ion pairs generated in matter and its fluctuation, following the passage of an ionizing particle or the absorption of an energy quantum. In the latter, the dissipation of energy released by a soft x-ray photon involves the photoelectric effect and its related processes: the Auger/Coster-Kronig transitions, fluorescence , electron shake-up and electron shake-off, as well as further gas ionization by the photo/Auger electrons. The x-ray energy absorption can be described by two energy-dependent parameters: the mean energy per ion pair (W_i) and the Fano factor (F). The mean energy per ion pair is defined by $W_i = \mathrm{E}/\bar{n}$ where E is the deposited energy and $\bar{n}$ is the mean number of induced electrons, while F characterizes the ionization fluctuation given by : $\sigma_{\bar{n}} = \sqrt{F\bar{n}}$.

The mean energy per ion pair was extensively studied both theoretically and experimentally [1], mainly for charged particles. However, only small number of measurements of F exist [2,3], mainly due to a lack of accurate experimental tools.

We report here on a new accurate experimental method for determination of F and W_i in the ultrasoft x-ray energy range. The method is applicable for all counting gases and their mixtures with noble gases. A complete description of this technique is presented elsewhere [4].

Ultrasoft x-rays are produced by a Particle-Induced X-ray Emission (PIXE) and are detected using an Electron Counting (EC) technique [5]. The electron swarms induced in a low-pressure gas are expanded while drifting under very low electric field towards a multiplication element. Electrons reach the multiplier in sequence and are therefore individually amplified. They are counted with very high efficiency and their number is proportional to the initial photon's energy. An example of

a fluorine-K (676 eV) induced electron pulse-trail is shown in fig. 1. A contour plot of the number of counted electron versus the electron trail length is shown in fig.2 for Be, C and Al lines. The additional time information helps resolving close lines.

In order to extract F and W_i we used a Monte-Carlo simulation, which accurately simulates all phenomena involved in the photoabsorption and electron transport multiplication and counting. A typical simulated electron pulse-trail is shown in fig. 1b. By correlating the experimental distributions of the number of counted electrons with the simulated ones, one can extract F and W_i. This is done by varying the simulation input parameters and testing the degree of agreement (χ^2 test) between the experimental and simulated counted electron distributions. An example of the good agreement between such experimental and simulated distributions is shown in fig.3.

Our results of F and W_i as a function of the photon energy for several gases and mixtures are presented in table. 1. In all gases, a tendency of decrease in F and W_i with increasing x-ray energy is observed. An increase of these parameters above the argon L-shell (≈ 250 eV) can be seen in the argon mixtures. An example of such behavior can be seen in fig.4 for i-C_4H_{10} and its mixture with argon. The increase of the W_i value above the argon L-shell energy is a result of the additional energy required to release an argon LMM-Auger electron compared to an M-electron. The increase in the F value is due to an opening of additional electron thermalization paths.

With its good accuracy, the method provides an excellent tool to study both the energy dependence of both parameters (F and W_i), as well as possible Penning and shell structure effects. We are currently investigating a new electron multiplier, based on a low-pressure microstrip amplification element [6], which will improve the accuracy of the method. We are currently studying F and W_i values in a large number of counting gases.

References

[1] International Commission on Radiation Units and Measurements, *Average Energy Required to Produce an Ion Pair*, ICRU Report No. 31, Washington, DC, 1979).

[2] D. Srdoc, B. Obelic, and I. Krajcar Bronic. *J.Phys B*, 20 (1987) 4473.

[3] T. H. V. T. Dias et al. *Nucl. Instr. and Meth.,* A307 (1991) 341.

[4] A. Pansky A. Breskin, R. Chechik, A new technique for studying the Fano factor and the mean energy per ion pair in counting gases, *to be published in the J. Appl. Phys, June 1996 issue.*

[5] A. Pansky A. Breskin, R. Chechik, and G. Malamud. Nucl. *Instr. and Meth.,* A330 (1993) 150.

[6] A. Breskin, E. Shefer, R. Chechik and A. Pansky. *Nucl. Instr. and Meth.,* A345 (1994) 205.

x-ray energy (eV)		108.5	183.5	277	676	1253	1486
C_2H_6	W_i	27.4(6)	28.0(4)	27.6(3)	27.2(5)		24.9(6)
	F	0.270(7)	0.280(7)	0.278(7)	0.260(10)		0.250(10)
Ar/C_2H_6(20:80)	W_i	27.4(6)	28.0(4)	27.6(3)	27.2(5)		24.9(6)
	F	0.270(7)	0.280(7)	0.278(7)	0.260(10)		0.250(10)
C_4H_{10}	W_i	28.0(4)	27.4(3)	27.9(3)	27.0(3)	25.6(3)	
	F	0.300(10)	0.285(9)	0.280(6)	0.265(9)	0.255(9)	
Ar/C_4H_{10}(20:80)	W_i	25.5(6)	26.3(4)	26.9(3)	26.4(5)	25.0(6)	
	F	0.275(15)	0.253(8)	0.265(7)	0.250(10)	0.250(10)	
DME-$(CH_3)_2O$	W_i	28.6(5)	28.5(4)	28.6(3)	28.4(4)	27.7(4)	
	F	0.340(15)	0.320(10)	0.315(10)	0.330(20)	0.285(20)	
Ar/DME (20:80)	W_i	26.8(5)	26.9(3)	27.7(3)	26.4(3)	26.8(5)	
	F	0.340(15)	0.300(10)	0.310(6)	0.330(10)	0.315(15)	

Table 1. Results of the mean energy per ion pair (W_i) and the Fano factor (F) extracted for various gases and gas mixtures by the electron counting technique. Errors are quoted in parenthesis.

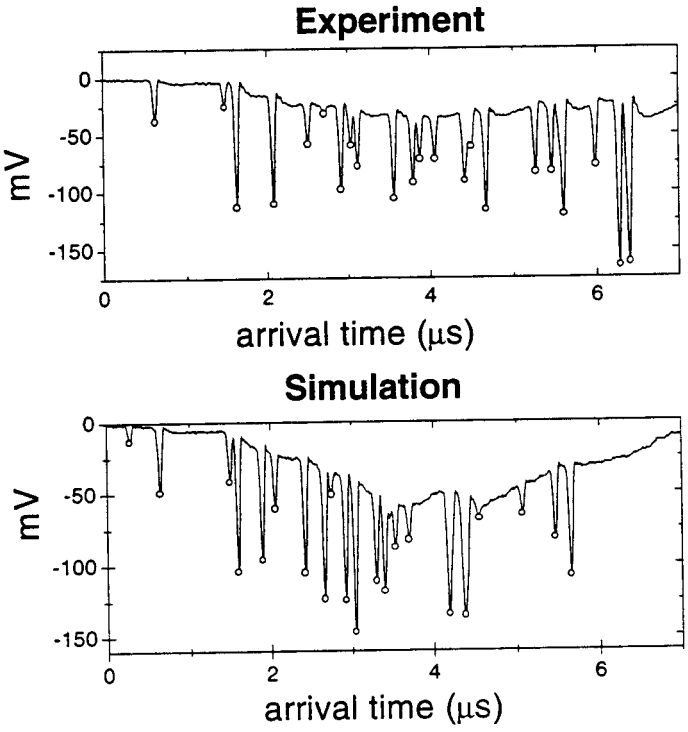

1. Typical 676 eV, Fluorine x-ray events: (a) a digitized experimental electron trail, (b) a simulated electron trail. Electron pulses recognized are circled in (a) and (b). $Ar/C_2H_6(20{:}80)$ at 20 Torr.

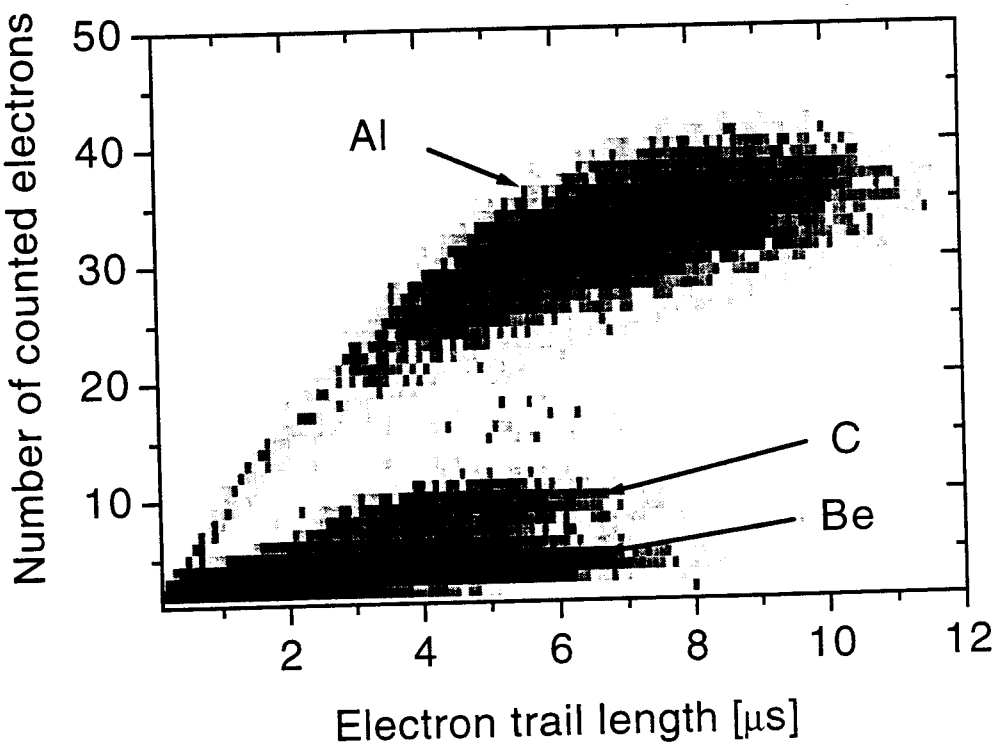

2. Contour plots of the counted number of electrons as a function of the pulse-trail length for Al-K, C-K and Be-K x-rays.

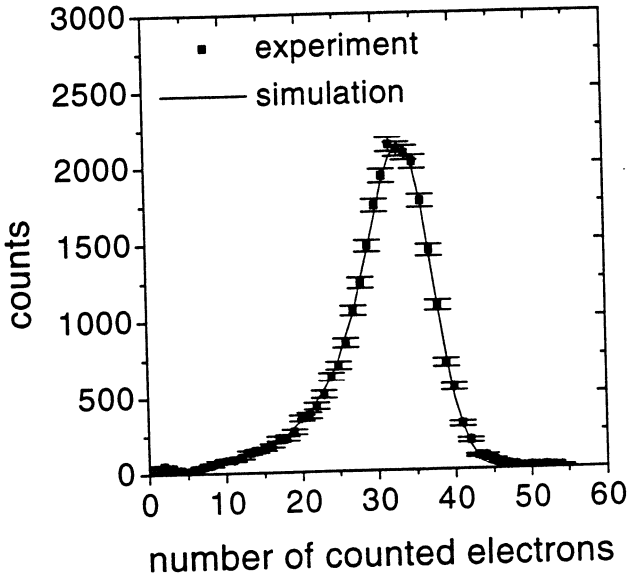

3. Distributions of experimental (squares) and simulation (lines) counted number of electrons. x-ray energy 1486 eV, Ar/C_2H_6 (20:80) at 20 Torr. Note that the simulation remarkably reproduces the experimental data.

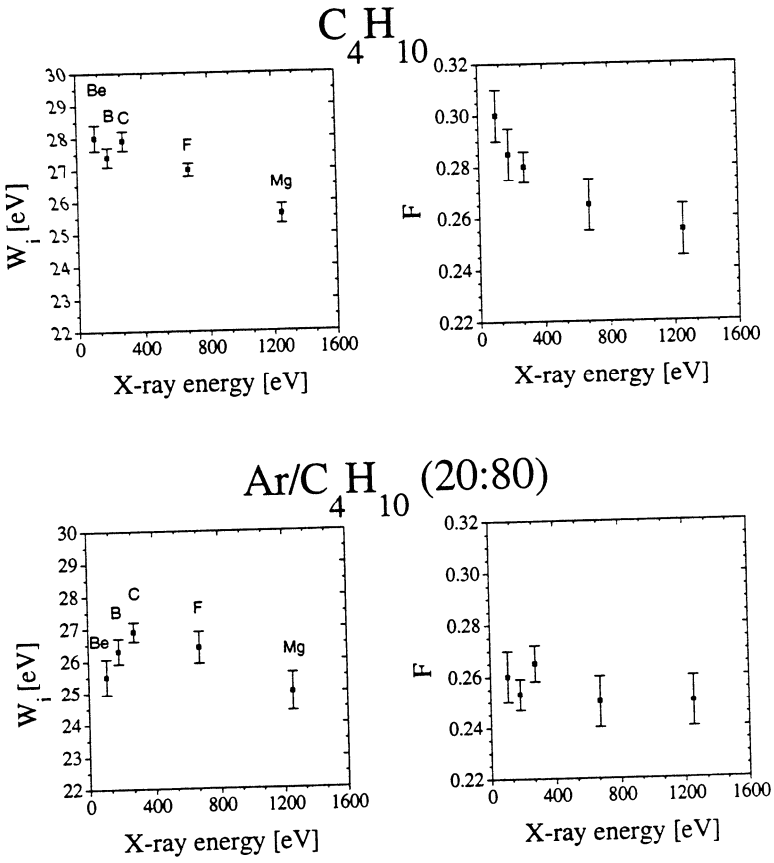

4. Extracted W_i and F values as function of x-ray energy for Ar/C_4H_{10} (20:80) and C_4H_{10}.

The Micro Sphere Plate: A novel electron multiplier

El-Mul Technologies Ltd.

Introduction

A Microsphere Plate (MSP) is a compact electron multiplier with temporal and spatial resolving power. It consists of glass beads 20 to 100 mm in diameter, sintered to form a thin, porous plate. The surface of the glass beads is covered with partially conductive, secondary-electron emissive material. The two faces of the plate are coated with conductive electrodes. Voltage applied between the two electrodes enables secondary electron multiplication in the gaps and passages between glass beads (See Fig. 1).

MSPs are used in vacuum systems for the detection of charged particles. Applications include particle-imaging, time-of-flight mass spectroscopy, particle counting, ion-beam monitoring, and electron microscopy. MSPs are also used for UV and X-ray imaging and in photomultipliers. MSPs are available in a variety of standard sizes and mounting configurations. The unique manufacturing process of MSPs makes it possible to fulfill almost any requirement for non-conventional size or shape.

MSP Operating Principle

The MSP is coated on both sides with conducting electrodes. A voltage of several thousand volts between the two electrodes establishes an electric field with an average direction normal to the faces of the plate. Primary electrons, ions or photons hitting the lower potential face of the MSP produce secondary electrons. These secondary electrons are accelerated by the electric field through the passages around the glass beads until the electrons hit a surface of a glass bead. In the collision more secondary electrons are generated. Each collision multiplies the number of electrons so that a large number of electrons emerge from the output side for each primary electron. The strip current, namely the flow of charge on the partially conductive surfaces of the glass beads, compensates for the electric charge drawn by the secondary electron emission process. The operation principle of MSPs is similar to that of Microchannel Plates (MCPs) except that the tortuous passages among the glass beads strongly inhibit ion feedback. Thus MSPs can operate at lower vacuum and provide higher gain.

MSP Characteristics

Vacuum requirements

MSPs operate in a wide-range of vacuum conditions, from 10^{-4} to 10^{-12} Torr. Ion feedback noise is not observed even under poor vacuum conditions.

Thickness

Single thickness (0.7 mm) MSP is suitable for analog measurements. It is also suitable for the measurement of pulses that include several particles (Time-of-flight mass spectrometry). The maximal operating voltage for a single thickness MSP is 3.0 kV. For pulse counting and for single particle detection, double thickness (1.4 mm) MSP is used. The maximal operating voltage for a double thickness MSP is 3.5 kV.

Amplification

Current amplification exceeds 10^6 and 10^7 for single and double thickness MSPs, respectively (See Fig. 2). At fixed voltage, the output current is generally a linear function of the input current. High output current, exceeding 10% of the strip current, results in gain saturation and deviation from linearity (See Fig. 3).

Pulse counting

For pulse counting applications and single particle detection, double thickness (1.4 mm) MSPs are preferable. Gain saturation in the passages among the glassbeads results in a well-pronounced peak in the output pulse height distribution (PHD), as shown in Fig, 4. The Pulse Height Ratio (PHR), defined as the peak FWHM divided by the peak value, is about 55% at bias voltage of 3.2 kV [Ref. 1, 2]. The noise PHD at 3.2 kV is exponential, with an average noise

pulse charge of about 2 pC. At this voltage, the average signal pulse charge (for a single incoming electron or photon) is about 15 pC. The width of the pulses is less than a nanosecond. Time resolution of less than 200 psec can be achieved.

Resistance

The resistance of single thickness MSPs ranges from 0.5 to 1.5 GigaΩ cm, whereas the resistance of double thickness MSPs ranges from 1.0 to 4.5 GigaΩ cm. The resistance is a decreasing function of the bias voltage and the temperature.

Aging

MSP aging causes gain reduction when operating at fixed voltage for a long time. Typically the gain is reduced to half its initial value after accumulated output charge of about 0.01 C/cm^2 emerges from the MSP. Fixed gain may be maintained for long periods by incrementing the MSP voltage.

Detection efficiency

MSPs are relatively insensitive to the incident angle of the detected particles (See Fig. 5). The incident angle is measured with respect to the MSP normal. No change in the PHD is observed at incident angles within this range [Ref. 1, 2]. For electrons, the maximal detection efficiency is obtained at 500 eV, as can be seen in Fig. 6.

Spatial resolution

The spatial resolution of MSPs is about 2 line-pair/mm. When a phosphor screen is positioned next to the MSP, the MSP pulses generate light spots on the screen (See Fig. 7). Single electrons generate 0.4 and 0.7 mm diameter light spots with single and double thickness MSP, respectively. The average lateral shift between the incident point of the incoming particle and the center of the light spot is 100 mm [Ref. 3].

Figure captions

1. Schematics of MSP multiplication chain
2. MSP amplification
3. MSP saturation characteristics
4. Double thickness MSP: Signal and noise PHD at 3.2 kV
5. MSP Sensitivity vs. Incident Angle of UV photons.
6. MSP sensitivity to electrons
7. Single electrons hitting an MSP, as seen at the phosphor screen

References

1. The Microsphere Electron Multiplier: Measurements and Modeling, A.S. Tremsin, J.F. Pearson, J.E. Lees and G.W. Fraser, SPIE Proc. 2518, “EUV, X-Ray and Gamma-Ray Instrumentation for Astronomy VI”, pp.384-396 (1995).
2. The Microsphere Plate: A New Type of Electron Multiplier, A.S. Tremsin, J.F. Pearson, J.E. Lees and G.W. Fraser, Nuclear Instruments and Methods in Physics Research A 368, pp. 719 (1996).
3. Imaging Performance of Microsphere Plates, J.S. Lapington, L.B.C. Worth and M.W. Trow, Proc. SPIE 2518 (1995).

For more Information please contact:

El-Mul Technologies Ltd.
Soreq, P.O. Box 571, Yavne 81104, Israel.
Tel: 972-8-9422677, Fax: 972-8-9422676, e-mail: 100274.16@compuserve.com

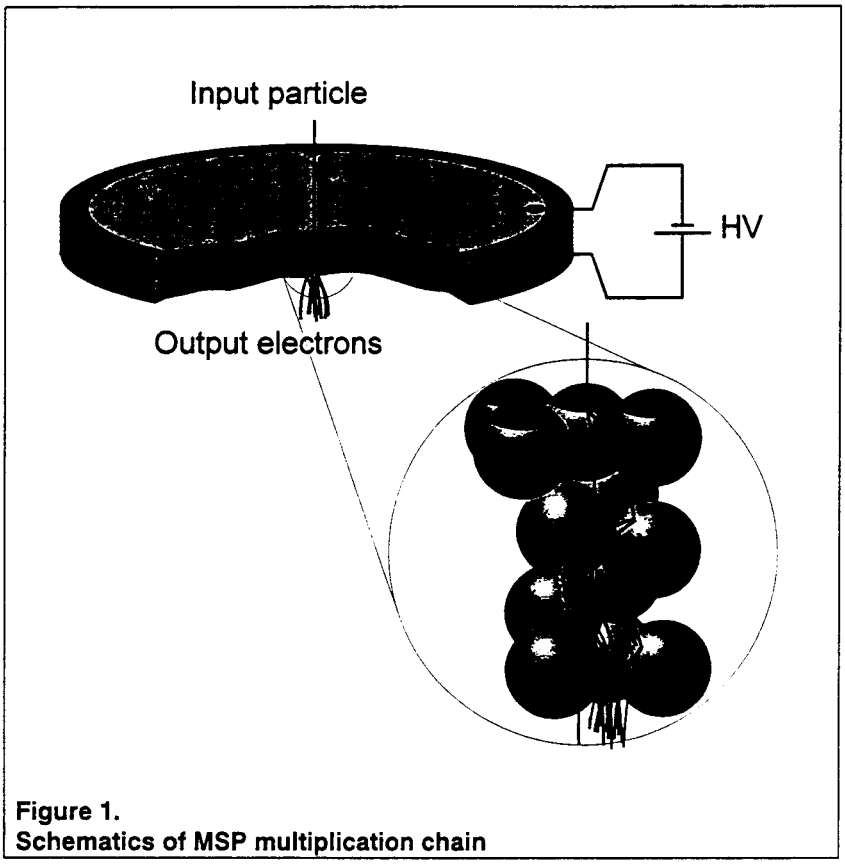

Figure 1.
Schematics of MSP multiplication chain

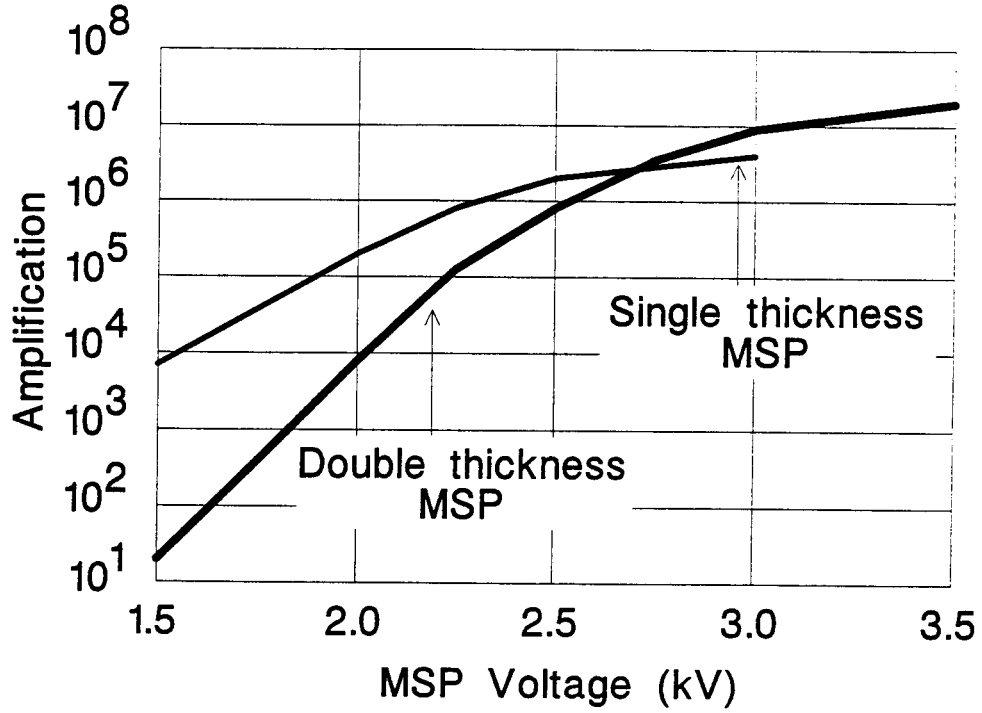

Figure 2.
MSP amplification

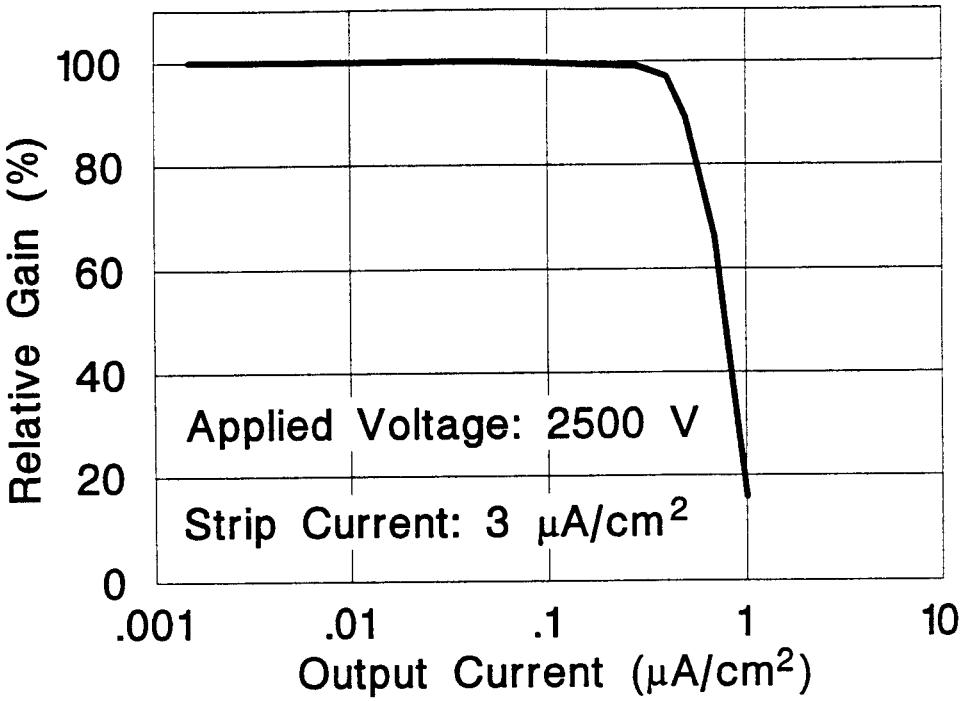

Figure 3.
MSP saturation characteristics

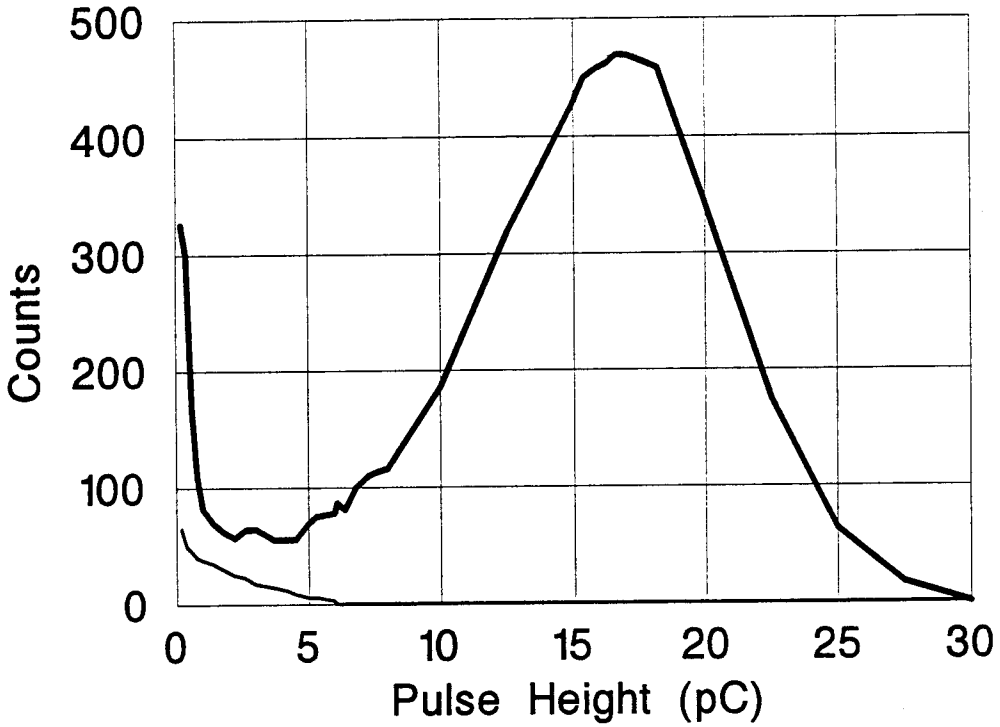

Figure 4.
Double thickness MSP: Signal and noise PHD at 3.2 kV

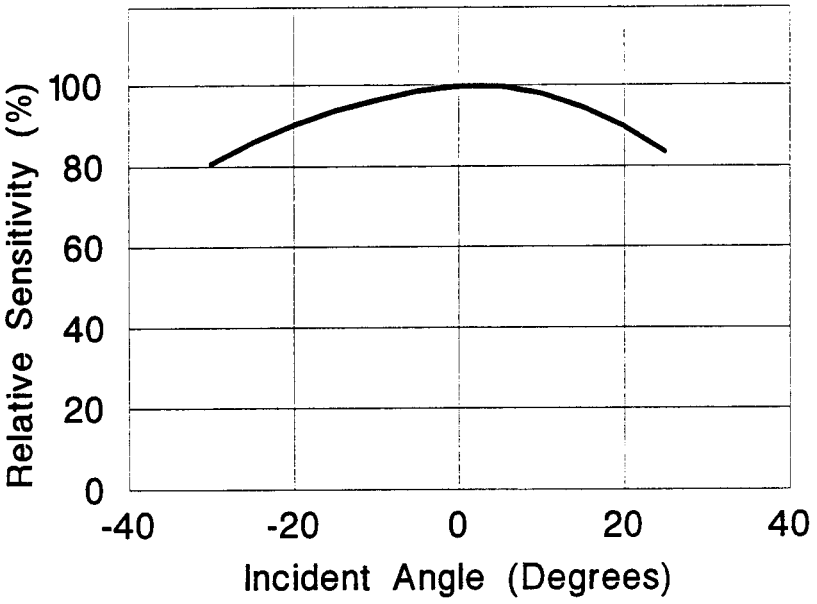

Figure 5.
MSP Sensitivity vs. Incident Angle of UV photons.

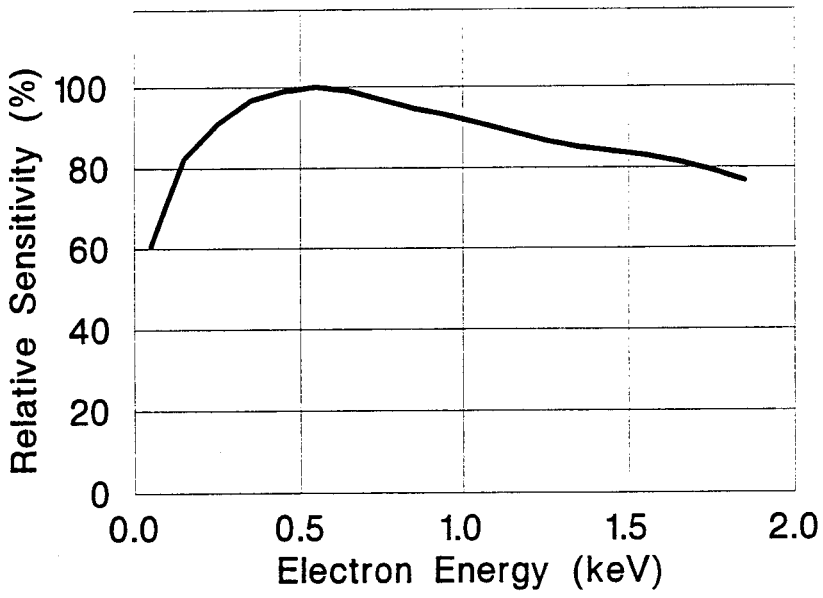

Figure 6.
MSP sensitivity to electrons

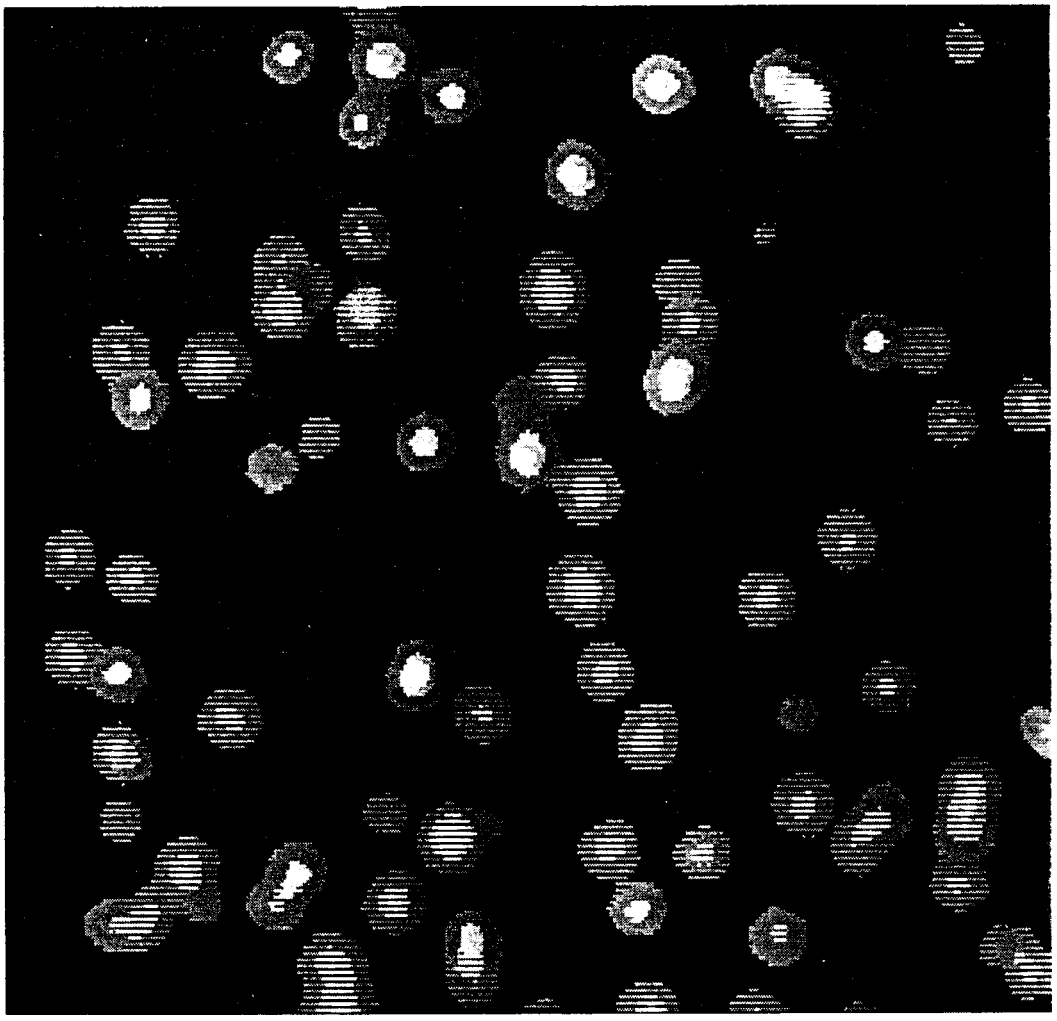

Figure 7.
Single electrons hitting an MSP, as seen at the phosphor screen

ETCHING OF COPPER COATED MYLAR TUBES WITH CF_4 GAS

Karl M. Ecklund, Keith W. Hartman, Michael J. Hebert, Stanley G. Wojcicki

Department of Physics, Stanford University
Stanford, California 94309

ABSTRACT

Using 5 mm diameter copper coated mylar straw tubes at a potential of 2.30 KV relative to a concentric 20 μm diameter gold-plated tungsten anode, it has been observed that with very low flow rates of CF_4-based gases the conductive copper cathode material may be removed entirely from the mylar surface.

1 Introduction

Experiment E871 in the B5 line of the Alternating Gradient Synchrotron at Brookhaven National Laboratory, is designed to search for very rare K_L decays with a single event sensitivity below 10^{-12}. For this search, the 24 GeV AGS proton beam producing $\sim 2 \times 10^8\, K_L^0$ per spill from a water-cooled platinum target is used. Expecting chamber rates of $\sim 200\ \mathrm{MHz/m^2}$ for this experiment, we selected 5 mm straw tubes with CF_4 based gases as a starting point for initial prototype studies. Our interest in CF_4 based gases lies primarily in their high drift velocities [1] and in their good aging characteristics [2–4].

2 Hardware Configuration

Our small test chamber is constructed of two 60 cm long, 5.0 mm diameter tubes each with a concentric 20 μm diameter gold-plated tungsten wire stretched to a tension of ~40 gm. The tubes

are made of 2-ply 0.5 mil mylar, the inner layer of which has a 1000 Å layer of copper vapor-deposited onto its inside surface. Cylindrical brass sleeves provide the mechanical support for and electrical contact between the straws and the endplates. Feedthroughs passing through the endplates and into the sleeves position the wire. Details of the endplate and feedthrough assembly will be provided upon request.

3 Copper Etching

Using two thin pieces of scintillator connected to phototubes, a trigger was defined with which the operating voltage of each gas was determined using a 5 mCi ^{90}Sr source. No difference in the operating voltage was observed between the two straw tubes with gases used in this study: $Ar\text{-}C_2H_6$ (50:50) and $CF_4\text{-}CH_4$ (30:70). The operating voltages for $Ar\text{-}C_2H_6$ and $CF_4\text{-}CH_4$ are 1.65 KV and 2.30 KV, respectively. Typically, the gas flow was about one volume change per minute.

The copper etching effect was first noticed accidentally: for a period of about ten hours, the gas $(CF_4\text{-}CH_4)$ flow was off while for one of the two straws, the HV was on. Visually, the difference between the two straws was striking: one was mostly transparent and the other appeared normal. A white powder was observed on the bottom of the etched tube. There are apparently no known volatile copper compounds.

Under more controlled circumstances, the etching effect was repeated with the undamaged straw. The basic procedure was simple: flow gas through the chamber, apply high volt age and note the current flowing between anode and cathode. At this point the gas flow was turned off and subsequent current measurements were made at regular time intervals.

With $CF_4\text{-}CH_4$ flowing at ~20 ml/min, no measurable current was flowing (with 10 nA sensitivity) at 2.30 KV. Approximately 90 minutes after turning the gas flow off, the chamber began drawing ~10 nA; after 2 hours it was drawing $5\mu A$. This was repeated many times.

When the chamber was drawing $5\mu A$ of current, a small amount of fresh gas (~2 ml) was introduced at which point the current dropped to less than 10 nA. About twenty minutes later, it was drawing measurable current again and after ~40 minutes, it was drawing 2 μA. This also was very repeatable.

Changing the gas to the $Ar\text{-}C_2H_6$ mixture and correspondingly reducing the operating voltage to 1.65 KV, the current at normal gas flow was less than 10 nA. Stopping gas flow, no measurable current was observed for 7 hours.

At this point we changed to pure CF_4 operating at the same voltage, namely 2.30 KV. Pure CF_4 began to draw current within a few minutes of turning off the gas flow and after about ten minutes the chamber was drawing ~60 μA; see Figure la. About an hour later, the current reached a maximum of ~180 μA and after about 90 minutes, it leveled off at around 140 μA. The straw

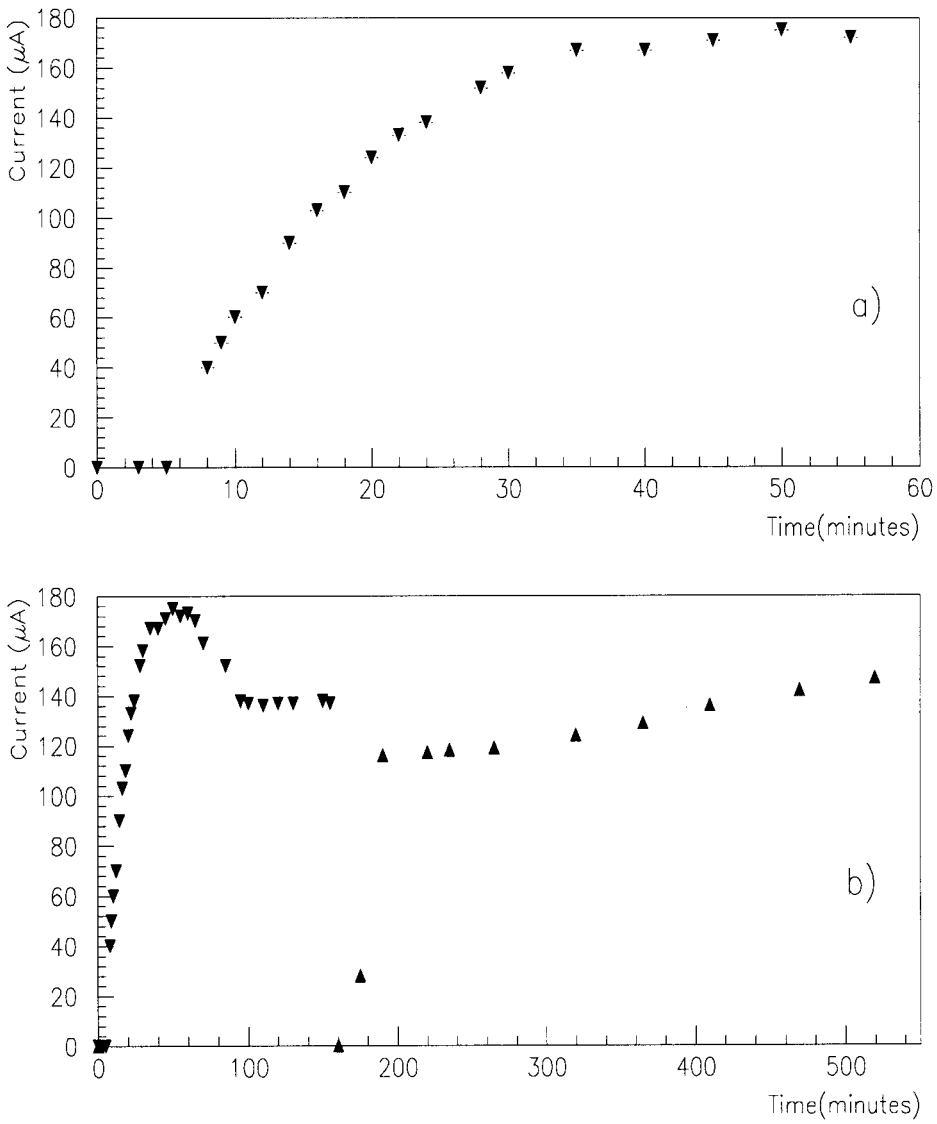

Figure 1: a) Short-term time dependence of current in straw #2 at 2.30 KV in pure CF_4 gas; b) Long-term time dependence; the copper began to thin visibly from the tube wall somewhere between 410-470 minutes on this plot. These data were taken over two days and the second set begins at t=160 minutes.

was turned off, flushed with fresh gas and the measurements started again at t=160 minutes in Figure 1b. About 310 minutes after beginning the second set of measurements, it became visibly apparent that the copper was being removed from the straw surface.

4 Suspected Mechanism

Under normal conditions CF_4 is considered a very inert gas; nonetheless, it is used[5,6] in the microelectronic fabrication industry as a component in the plasma etching of pure silicon and SiO_2. In one application of this process, CF_4 and either O_2 or H_2 are introduced into an evacuated chamber which is pumped with RF producing a plasma. In addition to ionizing the gas, the RF liberates fluorine radicals which react with the silicon to produce SiF_4. One may vary the etching rate of either the silicon or its oxide by introducing either O_2 or H_2.

Suspecting that O_2 was leaking into the chamber and reacting with the CF_4 in the high-field region near the anode wire, we built another small two-straw chamber for subsequent studies. This chamber was subjected to the same conditions as previously mentioned: pure CF_4 with HV at 2.30 KV and no gas flow. This chamber gave no indications of etching after 30 hours under these conditions. While introducing water vapor through a bubbler at room temperature did not induce etching, a pin hole in the straw tube wall did: the straw was drawing ~20 μA after about 20 minutes. Repeating the exercise in a volume of N_2, the chamber drew no current. Returning the chamber again to an atmosphere of air and raising the voltage to 2.30 KV with a fresh supply of CF_4 and zero flow rate, the copper began to visibly etch after about 4 hours in the region near the hole.

It was suggested[7] that the copper was being removed through a reaction resulting in CuF_2 as a final product. A possible reaction is:

$$CF_4 + O_2 \rightarrow CO_2 + 2F_2 \ .$$

The flourine is then free to react with the copper. As mentioned, a white powder was observed in the straw after the copper was removed and CuF_2 is known to be white in its crystalline form [8].

5 Summary

In the presence of O_2 in the high-field region of a straw drift chamber, CF_4-based gases will undergo a chemical reaction with the conducting copper coating of the straws. While it is, in general, not a good idea to introduce O_2 into a drift chamber, under certain conditions complete destruction of the chamber may result. A number of points may be made:

- CF_4 plus air in a straw chamber under high voltage removes the copper cathode material from the straw;
- ionizing radiation does not appear to be a factor;
- water vapor in the gas does not appear to be a factor;
- N_2 does not appear to be a factor.

For other reasons, the seven of eight straw chambers in experiment E871 at BNL were rebuilt for the 1996 run and to avoid problems arising from this effect two precautionary measures were taken: 1) the copper layer was increased from 1000 Å to 2000 Å; 2) all straws were individually pressure checked for leaks before installation. In addition to this, two operational changes were implemented: 1) gas flow rate was increased from 3 volume exchanges per day to 10 per day; 2) chamber voltage was ramped down between beam spills. The final chamber gas used in E871 was CF_4-C_2H_6 (50:50) with an operating voltage of 1950V (measured with an ^{55}Fe source, the gas gain is 8 x 10^4). Due to chamber capacitance, we were unable to ramp more than 100V down in the ~ 2 seconds available between the end of one AGS spill and the beginning of the next. As of this time, there is no indication of copper etching.

References

[1] Fisher, J., *et. al.,* NIM, **A238** (1987) 249.

[2] Henderson, R., *et. al.,* IEEE Trans. Nucl. Sci. **NS-35** (1988) 477.

[3] Openshaw, R. S., *et. al.,* IEEE Trans. Nucl. Sci. **NS-36** (1989) 567.

[4] Kadyk, J., *et. al.,* IEEE Trans. Nucl. Sci. **NS-37** (1990) 478.

[5] *A Guide to Reactive Ion Etching (1991)* March Instruments, Inc., 125-J Mason Circle, Concord, CA 94520.

[6] Poulsen, R. G., J. Vat. Sci. Technol., Vol. 14, No. 1, (1977) 266.

[7] Va'Vra, J., private communication.

[8] *CRC Handbook of Chemistry and Physics* 76th ed. (CRC Press, Inc.) 4-55.